

Black holes and global structures of spherical spacetimes in Horava-Lifshitz theoryJared Greenwald,^{1,*} Jonatan Lenells,^{2,†} J. X. Lu,^{3,‡} V. H. Satheeshkumar,^{1,§} and Anzhong Wang^{1,4,||}¹*GCAP-CASPER, Physics Department, Baylor University, Waco, Texas 76798-7316, USA*²*Mathematics Department, Baylor University, Waco, Texas 76798-7328, USA*³*Interdisciplinary Center for Theoretical Study, University of Science and Technology of China, Hefei, Anhui 230026, China*⁴*Department of Physics, Zhejiang University of Technology, Hangzhou 310032, China*

(Received 31 May 2011; published 18 October 2011)

We systematically study black holes in the Horava-Lifshitz theory by following the kinematic approach, in which a horizon is defined as the surface at which massless test particles are infinitely redshifted. Because of the nonrelativistic dispersion relations, the speed of light is unlimited, and test particles do not follow geodesics. As a result, there are significant differences in causal structures and black holes between general relativity (GR) and the Horava-Lifshitz theory. In particular, the horizon radii generically depend on the energies of test particles. Applying them to the spherical static vacuum solutions found recently in the nonrelativistic general covariant theory of gravity, we find that, for test particles with sufficiently high energy, the radius of the horizon can be made as small as desired, although the singularities can be seen, in principle, only by observers with infinitely high energy. In these studies, we pay particular attention to the global structure of the solutions, and find that, because of the foliation-preserving-diffeomorphism symmetry, $\text{Diff}(M, \mathcal{F})$, they are quite different from the corresponding ones given in GR, even though the solutions are the same. In particular, the $\text{Diff}(M, \mathcal{F})$ does not allow Penrose diagrams. Among the vacuum solutions, some give rise to the structure of the Einstein-Rosen bridge, in which two asymptotically flat regions are connected by a throat with a finite nonzero radius. We also study slowly rotating solutions in such a setup, and obtain all the solutions characterized by an arbitrary function $A_0(r)$. The case $A_0 = 0$ reduces to the slowly rotating Kerr solution obtained in GR.

DOI: [10.1103/PhysRevD.84.084040](https://doi.org/10.1103/PhysRevD.84.084040)

PACS numbers: 04.60.-m, 98.80.Bp, 98.80.Cq

I. INTRODUCTION

Horava-Lifshitz (HL) theory, proposed recently by Horava [1], and motivated by the Lifshitz theory of a scalar field with anisotropic scalings [2],

$$\mathbf{x} \rightarrow \ell \mathbf{x}, \quad t \rightarrow \ell^z t, \quad (z \neq 1), \quad (1.1)$$

has attracted a lot of attention, due to its several remarkable features. In particular, the effective speed of light in this theory diverges in the UV, which could potentially resolve the horizon problem without invoking inflation [3]. The spatial curvature is enhanced by higher-order curvature terms, and this opens a new approach to investigating both the flatness problem and bouncing universes [4–6]. In addition, in the superhorizon region, scale-invariant curvature perturbations can be produced without inflation [3,7–10]. The perturbations become adiabatic during slow-roll inflation driven by a single field, and the comoving curvature perturbation is constant [11]. For more details, we refer readers to [12–16].

Despite all these remarkable features, the theory is plagued with three major problems: ghosts, strong coupling, and instability. Although they are different, their

origins are the same: the breaking of the general covariance [17]. The preferred time that breaks general covariance leads to a reduced set of diffeomorphisms,

$$\tilde{t} = t - f(t), \quad \tilde{x}^i = x^i - \zeta^i(t, \mathbf{x}), \quad (1.2)$$

often denoted by $\text{Diff}(M, \mathcal{F})$. As a result, a spin-0 graviton appears. This mode is potentially dangerous and may cause the instability, ghost, and strong coupling problems, which could prevent the recovery of general relativity (GR) in the IR [12–16].

To resolve these problems, various modifications have been proposed. But, so far there are only two that seem to have the potential to solve these problems: One is due to Blas, Pujolas, and Sibiryakov (BPS) [18], who introduced a vector field

$$a_i = \partial_i \ln(N),$$

where N denotes the lapse function.¹ The other is due to Horava and Melby-Thompson (HMT) [22], in which the projectability condition

¹It is clear that the BPS model works only for the $N = N(t, x)$ case, in which the projectability condition $N = N(t)$ is broken. Otherwise, the vector field a_i will vanish identically. However, violation of the projectability condition often leads to the inconsistency problem [19]. But, as shown in [20], this is not the case in the BPS model. The inclusion of the vector field a_i gives rise to a proliferation of independent coupling constants [21], which could potentially limit the predictive powers of the theory.

*Jared_Greenwald@baylor.edu

†Jonatan_Lenells@baylor.edu

‡jxlu@ustc.edu.cn

§VH_Satheeshkumar@baylor.edu

||Anzhong_Wang@baylor.edu

$$N = N(t)$$

was assumed. In the HMT setup, the foliation-preserving-diffeomorphisms $\text{Diff}(M, \mathcal{F})$ are extended to include a local $U(1)$ symmetry, so that the total symmetry of the theory is enlarged to

$$U(1) \ltimes \text{Diff}(M, \mathcal{F}). \quad (1.4)$$

This symmetry is realized by introducing a $U(1)$ gauge field and a Newtonian prepotential, with which it can be shown that the spin-0 graviton is eliminated [22,23]. As a result, the instability problem does not exist in this setup. Another remarkable feature of the setup is that it forces the coupling constant λ to take exactly its relativistic value $\lambda_{\text{GR}} = 1$. Since both the ghost and strong coupling problems are due precisely to the deviation of λ from 1, this implies that these two problems are also resolved.

However, it has been argued [24] that the introduction of the Newtonian prepotential is so strong that actions with $\lambda \neq 1$ also have the $U(1) \ltimes \text{Diff}(M, \mathcal{F})$ symmetry. Although the spin-0 graviton is still eliminated for $\lambda \neq 1$, as shown explicitly by da Silva for de Sitter and anti-de Sitter backgrounds [24], and Huang and Wang for the Minkowski background [25], the ghost and strong coupling problems arise again. Indeed, it was shown [25] that to avoid the ghost problem, λ must satisfy the constraints

$$\lambda \geq 1 \quad \text{or} \quad \lambda < 1/3.$$

In addition, the coupling becomes strong for processes with energy higher than $M_{\text{pl}}|\lambda - 1|^{5/4}$ in the flat Friedmann-Robertson-Walker (FRW) background, and $M_{\text{pl}}|\lambda - 1|^{3/2}$ in a static weak gravitational field. It should be noted that for both cases to have nonvanishing gravitational perturbations, matter fields are necessarily present [25].

To solve the strong coupling problem [26], two different approaches have been proposed. One is the BPS mechanism [27], in which a UV cutoff M_* is introduced. By properly choosing the coupling constants involved in the theory, BPS showed that M_* can be lower than Λ_{SC} , where Λ_{SC} denotes the strong coupling energy scale of the theory. Then, for processes with energies higher than M_* , high-order derivative terms become important and need to be taken into account. The appearance of these terms change the scalings of the theory. In particular, all the irrelevant (nonrenormalizable) terms are turned into either marginal (strictly renormalizable) or relevant (super-renormalizable) ones. As a result, the would-be strong coupling scale Λ_{SC} disappears, due to the effects of high-order derivative terms, and the theory becomes renormalizable.² The other approach is to provoke the Vainshtein mechanism [30], as shown recently

²While this seems a very attractive mechanism, it turns out [28] that it cannot be applied to the Sotiriou-Visser-Weinfurter (SVW) generalization [29] (see also [3]) because of the instability of the spin-0 graviton [28]. However, in the HMT setup, the Minkowski spacetime is stable, and the BPS mechanism may now become available.

in the spherical static [12] and cosmological [28] spacetimes in the SVW setup [29].

In this paper, we leave the investigations of the strong coupling problem to a future study, and focus on another important issue: black holes in the HL theory. In the HL theory, due to the breaking of the general covariance, the dispersion relations of particles usually contain high-order momentum terms [12–16],

$$\omega_k^2 = m^2 + k^2 \left(1 + \sum_{n=1}^{z-1} \lambda_n \left(\frac{k}{M_n} \right)^{2n} \right), \quad (1.5)$$

for which the group velocity is given by [31]

$$v_k = \frac{k}{\omega} \left(1 + \sum_{n=1}^{z-1} (n+1) \lambda_n \left(\frac{k}{M_n} \right)^{2n} \right). \quad (1.6)$$

As an immediate result, the speed of light becomes unbounded in the UV. This makes the causal structure of the spacetimes quite different from that given in GR, where the light cone of a given point p plays a fundamental role in determining the causal relationship of p to other events [cf. Fig. 1]. However, once the general covariance is broken, the causal structure will be dramatically changed. For example, in the Newtonian theory, time is absolute and the speeds of the signals are not limited. Then, the causal structure of a given point p is uniquely determined by the time difference, $\Delta t \equiv t_p - t_q$, between the two events. In particular, if $\Delta t > 0$, the event q is to the past of p ; if $\Delta t < 0$, it is to the future; and if $\Delta t = 0$, the two events are simultaneous.

Another consequence of the breaking of the general covariance is that now free particles do not follow geodesics. This immediately makes all the definitions of black holes given in GR invalid [32–35]. To provide a proper definition of black holes, anisotropic conformal boundaries [36] and kinematics of particles [37] have been studied within the HL framework. In this paper, we shall adopt the approach of Kiritsis and Kofinas (KK) [38], where a horizon is defined as the infinitely redshifted two-dimensional (closed) surface of massless test particles. Clearly, such a definition reduces to that given in GR when the dispersion

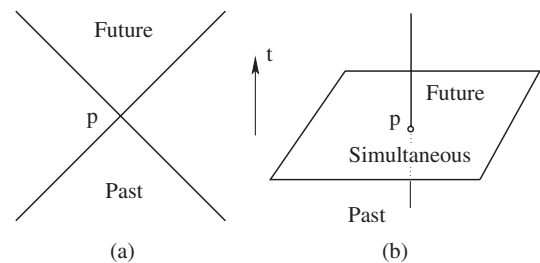


FIG. 1. (a) The light cone of the event p in special relativity. (b) The causal structure of the point p in Newtonian theory.

relation is relativistic [where $\lambda_n = 0$, as shown in Eq. (1.5)].

It should be noted that black holes in the HL theory with or without the projectability condition have been extensively studied, mainly using the definition borrowed directly from GR. In this paper, we shall show explicitly how these definitions are changed by considering some particular examples, found in the HMT setup with $\lambda = 1$.

Another interesting approach is the equivalence between the HL theory (without the projectability condition) and the Einstein-aether theory in the IR [39], where the former is equivalent to the latter for the case where the aether vector field u_μ is hypersurface-orthogonal.³ From such studies one already sees the difficulties in defining black holes, because of the fact that different modes may have different velocities even in the IR. In [39], black holes are defined to possess both a metric horizon and a spin-0 mode horizon. Since the equivalence holds only in the IR, it is still unclear how to extend such definitions to high-energy scales, where high-order curvature terms become important.

Specifically, the paper is organized as follows: In Sec. II, we briefly review the HMT setup (with $\lambda = 1$), while in Sec. III, we consider spherically symmetric black holes in the HL theory with the KK approach [38]. To keep our formulas as applicable as possible, in only this section we consider spacetimes that may or may not satisfy the projectability condition. We find that horizons are, in general, observer dependent, and that with sufficiently high energy, the radius of a horizon can be made arbitrarily small. This is consistent with the fact that the speed of light now becomes unbounded in the UV. In Sec. IV, we study all the vacuum diagonal ($N^i = 0$) solutions obtained in the HMT setup [22,40,41], paying particular attention to their global structure. Using the definition of horizons, we study their existence in various cases. It is remarkable that in some cases the structures of the Einstein-Rosen bridge exist, where a throat with finite nonzero radius connects two asymptotically flat regions. Because of the restricted diffeomorphisms (1.4), Penrose diagrams are not allowed. However, for the sake of comparison, we present the corresponding Penrose diagrams obtained by assuming that the general transformations are still allowed. In Sec. V, we study the nondiagonal ($N^i \neq 0$) vacuum solutions obtained in [40,41], while in Sec. VI, our main conclusions are presented. There are also two appendixes. In Appendix A, the 3-tensor F_{ij} for the spherical spacetimes is given, while in Appendix B, we study slowly rotating solutions in the HMT setup, and obtain all the solutions, which include the Kerr solution given in GR.

³In the spherically symmetric case, this is not a restriction as the aether field u_μ is now always hypersurface-orthogonal.

II. NONRELATIVISTIC GENERAL COVARIANT HL THEORY

The nonrelativistic general covariant HL theory is described by the action [22,23]

$$S = \zeta^2 \int dt d^3x N \sqrt{g} (\mathcal{L}_K - \mathcal{L}_V + \mathcal{L}_\varphi + \mathcal{L}_A + \zeta^{-2} \mathcal{L}_M), \quad (2.1)$$

where $g = \det g_{ij}$, and

$$\begin{aligned} \mathcal{L}_K &= K_{ij} K^{ij} - K^2, \\ \mathcal{L}_\varphi &= \varphi \mathcal{G}^{ij} (2K_{ij} + \nabla_i \nabla_j \varphi), \\ \mathcal{L}_A &= \frac{A}{N} (2\Lambda_g - R). \end{aligned} \quad (2.2)$$

Here Λ_g is a coupling constant and

$$\begin{aligned} K_{ij} &= \frac{1}{2N} (-\dot{g}_{ij} + \nabla_i N_j + \nabla_j N_i), \\ \mathcal{G}_{ij} &= R_{ij} - \frac{1}{2} g_{ij} R + \Lambda_g g_{ij}, \end{aligned} \quad (2.3)$$

where the Ricci terms all refer to the 3-metric g_{ij} . \mathcal{L}_M is the matter Lagrangian density, and \mathcal{L}_V is a Diff(Σ)-invariant local scalar functional. With the assumptions that the highest order derivatives are 6, and the parity is conserved, \mathcal{L}_V takes the general form [29]

$$\begin{aligned} \mathcal{L}_V &= \zeta^2 g_0 + g_1 R + \frac{1}{\zeta^2} (g_2 R^2 + g_3 R_{ij} R^{ij}) \\ &+ \frac{1}{\zeta^4} (g_4 R^3 + g_5 R R_{ij} R^{ij} + g_6 R^i_j R^j_k R^k_i) \\ &+ \frac{1}{\zeta^4} [g_7 R \nabla^2 R + g_8 (\nabla_i R_{jk}) (\nabla^i R^{jk})], \end{aligned} \quad (2.4)$$

where the coupling constants g_s ($s = 0, 1, 2, \dots, 8$) are all dimensionless. The relativistic limit in the IR requires $g_1 = -1$ and $\zeta^2 = 1/(16\pi G)$.

Then, it can be shown that the Hamiltonian and momentum constraints are given, respectively, by

$$\int d^3x \sqrt{g} (\mathcal{L}_K + \mathcal{L}_V - \varphi \mathcal{G}^{ij} \nabla_i \nabla_j \varphi) = 8\pi G \int d^3x \sqrt{g} J^t, \quad (2.5)$$

$$\nabla^j (\pi_{ij} - \varphi \mathcal{G}_{ij}) = 8\pi G J_i, \quad (2.6)$$

where

$$\begin{aligned} J^t &\equiv 2 \frac{\delta(N \mathcal{L}_M)}{\delta N}, \\ \pi_{ij} &\equiv -K_{ij} + K g_{ij}, \\ J_i &\equiv -N \frac{\delta \mathcal{L}_M}{\delta N^i}. \end{aligned} \quad (2.7)$$

Variation of the action (2.1) with respect to φ and A yields

$$\mathcal{G}^{ij}(K_{ij} + \nabla_i \nabla_j \varphi) = 8\pi G J_\varphi, \quad (2.8)$$

$$R - 2\Lambda_g = 8\pi G J_A, \quad (2.9)$$

where

$$J_\varphi \equiv -\frac{\delta \mathcal{L}_M}{\delta \varphi}, \quad J_A \equiv 2\frac{\delta(N\mathcal{L}_M)}{\delta A}. \quad (2.10)$$

On the other hand, the dynamical equations now read

$$\begin{aligned} \frac{1}{N\sqrt{g}}[\sqrt{g}(\pi^{ij} - \varphi \mathcal{G}^{ij})]_{,t} &= -2(K^2)^{ij} + 2KK^{ij} \\ &+ \frac{1}{N}\nabla_k[N^k \pi^{ij} - 2\pi^{k(i} N^{j)}] \\ &+ \frac{1}{2}(\mathcal{L}_K + \mathcal{L}_\varphi + \mathcal{L}_A)g^{ij} \\ &+ F^{ij} + F_\varphi^{ij} + F_A^{ij} + 8\pi G \tau^{ij}, \end{aligned} \quad (2.11)$$

where $(K^2)^{ij} \equiv K^{il}K_l^j$, $f_{(ij)} \equiv (f_{ij} + f_{ji})/2$, and

$$\begin{aligned} F^{ij} &\equiv \frac{1}{\sqrt{g}}\frac{\delta(-\sqrt{g}\mathcal{L}_V)}{\delta g_{ij}} = \sum_{s=0}^8 g_s \xi^{n_s} (F_s)^{ij}, \\ F_\varphi^{ij} &= \sum_{n=1}^3 F_{(\varphi,n)}^{ij}, \\ F_\varphi^i &= (K + \nabla^2 \varphi)\nabla^i \varphi + \frac{N^i}{N}\nabla^2 \varphi, \\ F_A^{ij} &= \frac{1}{N}[AR^{ij} - (\nabla^i \nabla^j - g^{ij}\nabla^2)A], \end{aligned} \quad (2.12)$$

where $n_s = (2, 0, -2, -2, -4, -4, -4, -4)$, and the geometric 3-tensors $(F_s)_{ij}$ and $F_{(\varphi,n)}^{ij}$ are given in [23]. The stress 3-tensor τ^{ij} is defined as

$$\tau^{ij} = \frac{2}{\sqrt{g}}\frac{\delta(\sqrt{g}\mathcal{L}_M)}{\delta g_{ij}}. \quad (2.13)$$

The matter quantities $(J^t, J^i, J_\varphi, J_A, \tau^{ij})$ satisfy the conservation laws

$$\begin{aligned} \int d^3x \sqrt{g} \left[\dot{g}_{kl} \tau^{kl} - \frac{1}{\sqrt{g}}(\sqrt{g}J^t)_{,t} \right. \\ \left. + \frac{2N_k}{N\sqrt{g}}(\sqrt{g}J^k)_{,t} - 2\dot{\varphi}J_\varphi - \frac{A}{N\sqrt{g}}(\sqrt{g}J_A)_{,t} \right] = 0, \end{aligned} \quad (2.14)$$

$$\begin{aligned} \nabla^k \tau_{ik} - \frac{1}{N\sqrt{g}}(\sqrt{g}J_i)_{,t} - \frac{J^k}{N}(\nabla_k N_i - \nabla_i N_k) - \frac{N_i}{N}\nabla_k J^k \\ + J_\varphi \nabla_i \varphi - \frac{J_A}{2N}\nabla_i A = 0. \end{aligned} \quad (2.15)$$

III. BLACK HOLES IN HL THEORY

KK considered a scalar field with a given dispersion relation $F(\zeta)$ [38]. In the geometrical optical approximations, ζ is given by $\zeta = g_{ij}k^i k^j$, where k_i denotes the 3-momentum of the corresponding spin-0 particle. With this approximation, the trajectory of a test particle is given by

$$\begin{aligned} S_p &\equiv \int_0^1 \mathcal{L}_p d\tau \\ &= \frac{1}{2} \int_0^1 d\tau \left[\frac{c^2 N^2}{e} \dot{t}^2 + e[F(\zeta) - 2\zeta F'(\zeta)] \right], \end{aligned} \quad (3.1)$$

where e is a one-dimensional einbein, and ζ is now considered as a functional of $t, x^i, \dot{t}, \dot{x}^i$, and e , given by the relation

$$\zeta[F'(\zeta)]^2 = \frac{1}{e^2} g_{ij}(\dot{x}^i + N^i \dot{t})(\dot{x}^j + N^j \dot{t}), \quad (3.2)$$

with $\dot{t} \equiv dt/d\tau$, etc. For details, we refer readers to [38].

It should be noted that KK obtained the above action starting from a scalar field. So, strictly speaking, it is valid only for spin-0 test particles. However, what is really important in their derivations is the dispersion relationship $F(\zeta)$. As shown in [42], a spin-2 particle has a similar dispersion relation. It is expected that spin-1 test particles, such as photons, should have a similar dispersion relation too [31,38]. Therefore, in the rest of this paper and without proof, we simply consider the action (3.1) to describe all massless test particles.

Spherically symmetric static spacetimes in the framework of the HMT setup were studied systematically in [40,41], and the metric for static spherically symmetric spacetimes that preserve the form of Eq. (1.2) with the projectability condition can be cast in the form [43]⁴

$$ds^2 = -c^2 dt^2 + e^{2\nu}(dr + e^{\mu-\nu} c dt)^2 + r^2 d^2\Omega, \quad (3.3)$$

where $d^2\Omega = d\theta^2 + \sin^2\theta d\phi^2$, and

$$\mu = \mu(r), \quad \nu = \nu(r), \quad N^i = \{ce^{\mu-\nu}, 0, 0\}. \quad (3.4)$$

The corresponding timelike Killing vector is $\xi = \partial_t$, and the diagonal case $N^r = 0$ corresponds to $\mu = -\infty$.

However, to study black hole solutions in a more general case, in this (and only in this) section, we also consider the case without the projectability condition, and write the metric as

$$ds^2 = -N^2 c^2 dt^2 + \frac{1}{f}(dr + N^r c dt)^2 + r^2 d^2\Omega, \quad (3.5)$$

where N, f , and N^r are all functions of r . Without loss of generality, in the rest of the paper we shall set $c = 1$, which

⁴Note the slight difference between the g_{rr} term defined here and the one defined in [41,43].

is equivalent to the coordinate transformations $x_0 = ct$, $\bar{N}^r = N^r/c$. Taking

$$F(\zeta) = \zeta^n \quad (n = 1, 2, \dots), \quad (3.6)$$

Eq. (3.2) yields

$$\zeta = \left(\frac{\dot{r} + N^r \dot{t}}{ne\sqrt{f}} \right)^{2/(2n-1)} \equiv \left(\frac{\mathcal{D}}{e^2} \right)^{1/(2n-1)}. \quad (3.7)$$

Inserting this into Eq. (3.1), we find that, for radially moving particles, \mathcal{L}_p is given by

$$\mathcal{L}_p = \frac{N^2}{2e} \dot{t}^2 + \frac{1}{2} (1 - 2n) e^{1/(1-2n)} \mathcal{D}^{n/(2n-1)}. \quad (3.8)$$

Then, from the equation $\delta \mathcal{L}_p / \delta e = 0$ we obtain

$$N^2 \dot{t}^2 - e^{2(n-1)/(2n-1)} \mathcal{D}^{n/(2n-1)} = 0. \quad (3.9)$$

On the other hand, since $\delta \mathcal{L}_p / \delta t = 0$, the Euler-Lagrange equation

$$\frac{\delta \mathcal{L}_p}{\delta t} - \frac{1}{d\tau} \left(\frac{\delta \mathcal{L}_p}{\delta \dot{t}} \right) = 0$$

yields

$$N^2 \dot{t} - e^{2(n-1)/(2n-1)} \frac{N^r}{\sqrt{f}} \mathcal{D}^{1/[2(2n-1)]} = eE, \quad (3.10)$$

where E is an integration constant, representing the total energy of the test particle.

To solve Eqs. (3.9) and (3.10), we first consider the case $n = 1$, which corresponds to the relativistic dispersion relation. From such considerations, we shall see how to generalize the definition of black holes given in GR to the HL theory, where n is generically different from 1, as required by the renormalizability condition in the UV.

A. $n = 1$

In this case, Eqs. (3.9) and (3.10) reduce, respectively, to

$$N^2 \dot{t}^2 - \mathcal{D} = 0, \quad (3.11)$$

$$N^2 \dot{t} - N^r \sqrt{\frac{\mathcal{D}}{f}} = eE. \quad (3.12)$$

Equation (3.11) simply tells us that now the particle moves along null geodesics. The above equations can be easily solved according to whether N^r vanishes or not.

1. $N^r = 0$

When $N^r = 0$, from Eq. (3.11) we find

$$dt = \pm \frac{dr}{N\sqrt{f}}, \quad (3.13)$$

where “+” (“−”) corresponds to outgoing (ingoing) light rays. If f has an a th order zero and N^2 a b th order zero at a surface, say, $r = r_g$, that is,

$$f = f_0(r)(r - r_g)^a, \quad N = N_0(r)(r - r_g)^{b/2}, \quad (3.14)$$

where $N_0(r_g) \neq 0$ and $f_0(r_g) \neq 0$, then from the above equations we find that, in the neighborhood of $r = r_g$,

$$t \simeq t_0 \pm \frac{1}{N_0\sqrt{f_0}} \begin{cases} \frac{2}{2-(a+b)} (r - r_g)^{1-(a+b)/2} & a + b \neq 2 \\ \ln|r - r_g| & a + b = 2. \end{cases} \quad (3.15)$$

Therefore, when

$$a + b \geq 2, \quad (n = 1), \quad (3.16)$$

the time t becomes unbounded, $|t| \sim \infty$, as $r \rightarrow r_g$. Hence, the light rays are infinitely redshifted at this surface. This indicates that an event horizon might exist at $r = r_g$, provided that the spacetime has no curvature singularity there. A simple example is the Schwarzschild solution, $N^2 = f = (r - r_g)/r$, which is also a solution of the HL theory without the projectability condition, but with the detailed balance condition softly broken [44], and for which we have $a = b = 1$. Clearly, it satisfies the above condition with the equality, so $r = r_g$ indeed defines a horizon.

2. $N^r \neq 0$

When $N^r \neq 0$, Eq. (3.11) yields

$$t = t_0 + \int \frac{\epsilon dr}{N\sqrt{f} - \epsilon N^r}, \quad (3.17)$$

where $\epsilon = +1$ ($\epsilon = -1$) corresponds to outgoing (ingoing) light rays. If

$$H(r) \equiv N\sqrt{f} - \epsilon N^r \quad (3.18)$$

has δ th order zero at r_g ,

$$H(r) = H_0(r)(r - r_g)^\delta, \quad (3.19)$$

with $H_0(r_g) \neq 0$, we find that in the neighborhood $r = r_g$ Eq. (3.17) yields

$$t = t_0 + \frac{\epsilon}{H_0(r_g)} \frac{1}{1 - \delta} \begin{cases} (r - r_g)^{1-\delta} & \delta \neq 1 \\ \ln(r - r_g) & \delta = 1. \end{cases} \quad (3.20)$$

Clearly, when

$$\delta \geq 1, \quad (n = 1), \quad (3.21)$$

$|t|$ becomes unbounded as $r \rightarrow r_g$, and an event horizon might exist.

The Schwarzschild solution in the Painlevé-Gullstrand coordinates [45] is given by

$$N_{\text{Sch}}^2 = f_{\text{Sch}} = 1, \quad N_{\text{Sch}}^r = \epsilon_1 \sqrt{\frac{r_g}{r}}, \quad (3.22)$$

where $\epsilon_1 = \pm 1$. As shown in [40,41], this is also a vacuum solution of the HL theory in the HMT setup [22]. Then, we find that $H(r) = 1 - \epsilon_1 \epsilon \sqrt{r_g/r}$. Thus, for the solution with $\epsilon_1 = +1$, the time of the outgoing null rays, measured by asymptotically flat observers, becomes unbounded at r_g , and for the solution with $\epsilon_1 = -1$, the time of the ingoing null rays becomes unbounded. Therefore, an event horizon is indicated to exist at $r = r_g$ in both cases.

In review of the above, KK generalized the notion of black holes defined in GR to the case of a nonstandard dispersion relation [38]. In particular, a horizon is defined as a surface on which light rays are infinitely redshifted. It should be noted that this redshift should be understood as measured by asymptotically flat observers, at which $N(r \gg r_g) \simeq 1$ and $N^r(r \gg r_g) \simeq 0$, with r being the geometric radius, $r = \sqrt{A/4\pi}$, of the 2-sphere: $t, r = \text{Constants}$, where A denotes the area of the 2-sphere.

B. $n \geq 2$

In this case, eliminating e from Eqs. (3.9) and (3.10) we find that

$$X^n - p(r)X - q(r, E) = 0, \quad (3.23)$$

where

$$X \equiv \left(\frac{\sqrt{\mathcal{D}}}{t}\right)^{1/(n-1)} = \left(\frac{|r' + N^r|}{n\sqrt{f}}\right)^{1/(n-1)},$$

$$p(r) \equiv \frac{N^r}{\sqrt{f}}, \quad q(r, E) \equiv EN^{1/(n-1)}, \quad (3.24)$$

with $r' \equiv \dot{r}/t = dr/dt$. To solve the above equation, again it is found convenient to consider the cases $N^r = 0$ and $N^r \neq 0$ separately.

I. $N^r = 0$

When $N^r = 0$, Eq. (3.23) has the solution

$$t = t_0 + \epsilon \int \frac{dr}{nE^{(n-1)/n}\sqrt{f}N^{1/n}}, \quad (3.25)$$

where $\epsilon = +1$ corresponds to outgoing rays, and $\epsilon = -1$ to ingoing rays. Thus, if f has an a th order zero and N^2 a b th order zero at $r = r_g$, as given by Eq. (3.14), we have $\sqrt{f}N^{1/n} \sim (r - r_g)^{(a+b/n)/2}$. Then, from the above, we find that the time t , measured by asymptotically flat observers, becomes infinitely large at $r = r_g$, provided that [38]

$$a + \frac{b}{n} \geq 2. \quad (3.26)$$

For the solutions with the projectability condition ($N = 1, b = 0$), this is possible only when $a \geq 2$.

Considering again the Schwarzschild solution, $N^2 = f = (r - r_g)/r$, one finds that this does not satisfy the condition (3.26) with $n \geq 2$. Therefore, the Schwarzschild black hole in GR is no longer a black hole in the HL theory, because of the nonrelativistic dispersion relations (1.5). This is expected, since even in GR when quantum effects are taken into account, such as the Hawking radiation, classical black holes are no longer black.

2. $N^r \neq 0$

In this case, let us consider an ingoing ray $r' < 0$. Suppose there is a horizon located at $r = r_H$. Then $r'(r) \simeq 0$ as we approach the horizon. Thus, if $N^r > 0$ and bounded away from zero, $(r' + N^r)$ will also be positive, when the ray is sufficiently near the horizon. Conversely, if $N^r < 0$ and bounded away from zero, then $(r' + N^r)$ will be negative sufficiently near the horizon. Defining H by $H(r, E) \equiv r'$, we find that for an ingoing ray near the horizon, we have

$$t = t_0 + \int \frac{dr}{H(r, E)}, \quad (3.27)$$

$$H(r, E) = \epsilon n \sqrt{f} X^{n-1} - N^r, \quad (3.28)$$

where

$$\epsilon = \begin{cases} 1 & N^r > 0 \\ -1 & N^r < 0. \end{cases} \quad (3.29)$$

Dividing (3.23) by X and solving for X^{n-1} , we obtain

$$X^{n-1} = \frac{N^r}{\sqrt{f}} + \frac{EN^{1/n-1}}{X}.$$

Substituting this into (3.28), we find

$$H = (\epsilon n - 1)N^r + \epsilon n \sqrt{f} \frac{EN^{1/n-1}}{X}. \quad (3.30)$$

It follows that if H has a zero at $r = r_H$, then

$$X|_{r=r_H} = -\frac{\epsilon n \sqrt{f} EN^{1/n-1}}{(\epsilon n - 1)N^r}. \quad (3.31)$$

The expression on the right-hand side is positive (negative) for $\epsilon = -1$ ($\epsilon = 1$). Thus, H can have a zero only if $\epsilon = -1$. Thus, we will henceforth consider only this case. Differentiation of (3.30) with respect to r yields

$$H'(r) = -(n+1)N^{r'} - n\sqrt{f} \frac{EN^{(1/n-1)-1}}{(n-1)X} N' - n \frac{EN^{(1/n-1)}}{2\sqrt{f}X} f' + n\sqrt{f} \frac{EN^{(1/n-1)}}{X^2} X'. \quad (3.32)$$

On the other hand, differentiation of (3.23) with respect to r yields

$$X'(r) = \frac{1}{nX^{n-1} - \frac{N^r}{\sqrt{f}}} \left[\left(\frac{1}{\sqrt{f}} \frac{dN^r}{dr} - \frac{N^r}{2f^{3/2}} \frac{df}{dr} \right) X + \frac{EN^{(1/n-1)-1}}{n-1} \frac{dN}{dr} \right]. \quad (3.33)$$

Substituting the above into Eq. (3.32), we find that

$$H'(r)|_{r=r_H} = -\frac{n+1}{2} \left(\frac{H_1}{H_2} - \frac{N^r f'}{f} + \frac{2N^r N'}{N-nN} + 2N^{r'} \right), \quad (3.34)$$

where

$$H_1 \equiv 2E(n+1)fN^r N' + E(n-1)nN(N^r f' - 2fN^{r'}),$$

$$H_2 \equiv (n-1)n f N \left[E + (n+1)N^{1/1-n} \left(\frac{En\sqrt{f}N^{1/n-1}}{(-n-1)N^r} \right)^n \right]. \quad (3.35)$$

If H has a zero of order $\delta > 0$ at r_H , we can write it in the form

$$H(r) = H_0(r_H)(r - r_H)^\delta + \dots, \quad (3.36)$$

as $r \rightarrow r_H$, where $H_0(r_H) \neq 0$. Therefore,

$$H'(r)|_{r=r_H} = \begin{cases} 0 & \delta > 1 \\ H_0(r_H) & \delta = 1 \\ \pm\infty & 0 < \delta < 1. \end{cases} \quad (3.37)$$

Now $t \rightarrow \infty$ as $r \rightarrow r_H^+$ if and only if

$$\delta \geq 1, \quad (3.38)$$

which happens if and only if $dH/dr|_{r=r_H}$ is finite. This gives an explicit condition on f, N, N', E, n for the blowup of t at r_H .

It should be noted that r_H usually depends on the energy E of the test particles, as can be seen from the above and specific examples considered below.

Case $n = 2$: In this case, we have

$$H'(r)|_{r=r_H} = \frac{H_3}{2N[4EfN + 3(N^r)^2]}, \quad (3.39)$$

where

$$H_3 \equiv 3[4EN^2(N^r f' - 2fN^{r'}) + 8EfNN^r N' - 3(N^r)^3 N'], \quad (n = 2). \quad (3.40)$$

Again, for the Schwarzschild solution (3.22), we have

$$X(r) = \frac{1}{2} \left(-\sqrt{\frac{r_g}{r}} + \frac{\sqrt{4Er + r_g}}{\sqrt{r}} \right), \quad (3.41)$$

$$H(r) = \frac{-3\sqrt{r_g(4Er + r_g)} + 4Er + 3r_g}{\sqrt{r r_g} - \sqrt{r(4Er + r_g)}},$$

so that $H(r) = 0$ has the solution

$$r_H = \frac{3r_g}{4E}, \quad (n = 2), \quad (3.42)$$

at which we have

$$H'(r_H) = -\frac{2E^{3/2}}{\sqrt{3}r_g}. \quad (3.43)$$

Then, according to Eq. (3.37), we have $\delta = 1$; i.e., t diverges logarithmically as $r \rightarrow r_H^+$. Therefore, in this case there does exist a horizon. But, its location depends on the energy E of the test particle, and approaches zero when $E \gg r_g$. This is understandable, as the speed of light is unbounded in the UV, and, in principle, the singularity located at $r = 0$ can be seen by asymptotically flat observers, as long as the light rays sent by the observers have sufficiently high energies.

Case $n = 3$: In this case, we have

$$X^3 - p(r)X - q(r, E) = 0. \quad (3.44)$$

Assuming that $H(r) = 0$ has a real and positive root r_H , we find that

$$H'(r)|_{r=r_H} = \frac{H_4}{3N(27E^2 f^{3/2} N - 16(N^r)^3)}, \quad (3.45)$$

where

$$H_4 \equiv 162E^2 \sqrt{f} N^2 N^r f' + 32(N^r)^4 N' - 162E^2 f^{3/2} N(2NN^r - N^r N'). \quad (3.46)$$

For the Schwarzschild solution (3.22), we have $p(r) = -\sqrt{r_g/r}$ and $q(r, E) = E$. Then, we find that

$$X^3 + \sqrt{\frac{r_g}{r}} X - E = 0, \quad (3.47)$$

$$H(r) = 4\sqrt{\frac{r_g}{r}} - \frac{3E}{X}, \quad (3.48)$$

from which we find that $H(r) = 0$ has a solution,

$$r_H = r_g \left(\frac{16}{27E^2} \right)^{2/3}, \quad (n = 3), \quad (3.49)$$

which also depends on E , and approaches zero as $E \rightarrow \infty$. Substituting r_H into Eq. (3.45), we find $H'(r_H) = -27E^2/(16r_g)$. That is, the hypersurface $r = r_H$ is also an observer-dependent horizon in the case $n = 3$, and the radius of the horizon is inversely proportional to the energy of the test particle. For $E \gg r_g$, we have $r_H \approx 0$.

Another (simpler) consideration for the existence of the horizon is given as follows: First, from Eq. (3.24) we find that

$$X = \left(\frac{|r' + N^r|}{n\sqrt{f}} \right)^{1/(n-1)} \simeq \left(\frac{\epsilon N^r}{n\sqrt{f}} \right)^{1/(n-1)} \left(1 + \frac{H}{(n-1)N^r} \right), \quad (3.50)$$

for $r \simeq r_H$. Inserting it into Eq. (4.2), we have, to leading order,

$$\begin{aligned} & \left(1 + \frac{EN^{1/(n-1)}}{(n-1)\left(\frac{\epsilon N^r}{n\sqrt{f}}\right)^{n/(n-1)}} \right) H(r, E) \\ &= (\epsilon n - 1)N^r \left(1 + \frac{EN^{1/(n-1)}}{(\epsilon n - 1)\left(\frac{\epsilon N^r}{n\sqrt{f}}\right)^{n/(n-1)}} \right). \end{aligned} \quad (3.51)$$

Then, we obtain

$$\frac{EN^{1/(n-1)}}{(n+1)\left(\frac{-N^r(r)}{n\sqrt{f(r)}}\right)^{n/(n-1)}} \Big|_{r=r_H} = 1. \quad (3.52)$$

Given this, we can further simplify Eq. (3.51) to

$$\begin{aligned} & \frac{2n}{n-1} H(r, E) \\ &= -(n+1)N^r(r_H) \left(1 - \frac{EN^{1/(n-1)}(r)}{(n+1)\left(\frac{-N^r(r)}{n\sqrt{f(r)}}\right)^{n/(n-1)}} \right). \end{aligned} \quad (3.53)$$

Then, using Eq. (3.36), we have the following constraint for N , N^r , f to satisfy so that a horizon can indeed exist,

$$\begin{aligned} & \frac{EN^{1/(n-1)}(r)}{(n+1)\left(\frac{-N^r(r)}{n\sqrt{f(r)}}\right)^{n/(n-1)}} \\ &= 1 + \frac{2nH_0(r_H)}{(n^2-1)N^r(r_H)}(r-r_H)^\delta + \dots \end{aligned} \quad (3.54)$$

This equation can first be used to determine r_H and then δ , once N , N^r , and f are given. To illustrate how to use it, let us consider the Schwarzschild metric (3.22). For $n=2$, r_H can be obtained simply from the above, and is given exactly by Eq. (3.42), for which we have

$$\frac{EN^{1/(n-1)}(r)}{(n+1)\left(\frac{-N^r(r)}{n\sqrt{f(r)}}\right)^{n/(n-1)}} \simeq 1 + \frac{r-r_H}{r_H}, \quad (3.55)$$

that is, $\delta = 1$.

For $n=3$, from Eq. (3.52) we find that r_H is given by Eq. (3.49), and

$$\begin{aligned} & \frac{EN^{1/(n-1)}(r)}{(n+1)\left(\frac{-N^r(r)}{n\sqrt{f(r)}}\right)^{n/(n-1)}} = \frac{3^{3/2}E_r^{3/4}}{4r_g^{3/4}} \\ & \simeq 1 + \frac{3}{4r_H}(r-r_H) + \dots \end{aligned} \quad (3.56)$$

Therefore, in this case we have $\delta = 1$, too.

It should be noted that in the above analysis, we assumed that $F(\zeta) = \zeta^n$. In more realistic models, the dispersion relation is a polynomial of ζ , as shown by Eq. (1.5), or more specifically,

$$F(\zeta) = \zeta + \frac{\zeta^2}{M_A^2} + \frac{\zeta^4}{M_B^4} + \dots, \quad (3.57)$$

where M_A and M_B are the energy scales, which can be significantly different from the Planck one [27]. Therefore, for observers in low-energy scales, where $\zeta \ll M_A, M_B$, the first term dominates, and some solutions, including the Schwarzschild solution, look like black holes, as shown in the case $n=1$. But, for observers with high energies, those solutions may not be black holes any longer. Even if they are, their horizons, in general, are observer dependent, as shown in the cases $n=2$ and $n=3$ explicitly for the Schwarzschild solution. To illustrate the main properties of the dispersion relation (3.57), we shall consider the case where only the first two terms are important.

C. Trajectories of test particles with the dispersion relation $F(\zeta) = \zeta + \zeta^2/M_A^2$

For the sake of simplicity, we restrict ourselves to the case $N^r = 0$. Substituting

$$F(\zeta) = \zeta + \frac{\zeta^2}{M_A^2} \quad (3.58)$$

into Eq. (3.2), we find

$$\zeta \left(1 + \frac{2\zeta}{M_A^2} \right)^2 = \frac{\dot{r}^2}{e^2 f}. \quad (3.59)$$

Solving this equation directly for ζ yields a very complicated expression, and it is not clear how to proceed along this direction. Instead, we note that our goal is to find the analog of Eq. (3.9), i.e. of the equation $\delta \mathcal{L}_p / \delta e = 0$, where

$$\begin{aligned} \mathcal{L}_p &= \frac{1}{2} \left(\frac{N^2}{e} \dot{r}^2 + e[F(\zeta) - 2\zeta F'(\zeta)] \right) \\ &= \frac{1}{2} \left(\frac{N^2}{e} \dot{r}^2 - e \left[\zeta + \frac{3\zeta^2}{M_A^2} \right] \right). \end{aligned} \quad (3.60)$$

Thus, we will first calculate $\delta \zeta / \delta e$, implicitly by applying $\delta / \delta e$ to both sides of (3.59), which yields

$$\frac{\delta \zeta}{\delta e} = - \frac{2M_A^4 \dot{r}^2}{e^3 f (M_A^4 + 8M_A^2 \zeta + 12\zeta^2)}. \quad (3.61)$$

Substituting this into the expression

$$\frac{\delta \mathcal{L}_p}{\delta e} = \frac{1}{2} \left(- \frac{N^2}{e^2} \dot{r}^2 - \left[\zeta + \frac{3\zeta^2}{M_A^2} \right] - e \left[\frac{\delta \zeta}{\delta e} + \frac{6\zeta}{M_A^2} \frac{\delta \zeta}{\delta e} \right] \right),$$

we find the following analog of Eq. (3.9),

$$\zeta(e^2 M_A^2 + 2N^2 i^2) + 5e^2 \zeta^2 + \frac{6e^2 \zeta^3}{M_A^2} + M_A^2 \left(N^2 i^2 - \frac{2i^2}{f} \right) = 0, \quad (3.62)$$

where ζ is given implicitly by Eq. (3.59). Note that in the limit $M_A \rightarrow \infty$, the above equation reduces precisely to Eq. (3.9) for $F(\zeta) = \zeta$ and $N^r = 0$, as expected.

On the other hand, the analog of Eq. (3.10) is simply

$$N^2 i = eE. \quad (3.63)$$

Using Eqs. (3.59) and (3.63) to eliminate i and \dot{i} from Eq. (3.62), we find⁵

$$\frac{\delta \mathcal{L}_p}{\delta e} = \frac{1}{2} \left(\zeta + \frac{\zeta^2}{M_A^2} - \frac{E^2}{N^2} \right) = 0.$$

Solving this equation for ζ , we infer that

$$\zeta = -\frac{M_A^2}{2} + \frac{M_A}{2N} \sqrt{4E^2 + M_A^2 N^2}.$$

Substitution of this expression into Eq. (3.62) yields

$$\frac{M_A(N^2(\frac{2i^2}{e^2 f} + M_A^2) + 4E^2)}{N\sqrt{4E^2 + M_A^2 N^2}} - \frac{N^2 i^2}{e^2} - \frac{3E^2}{N^2} - M_A^2 = 0. \quad (3.64)$$

Replacing e by $N^2 i/E$ and then solving the resulting equation for i/\dot{i} , we find⁶

$$\frac{i^2}{\dot{i}^2} = \frac{fN(4E^2 + M_A^2 N^2)(\sqrt{4E^2 + M_A^2 N^2} - M_A N)}{2E^2 M_A}.$$

Thus, the trajectory is given by

$$t = t_0 + \int \frac{dr}{H(r, E)}, \quad (3.65)$$

where

$$H(r, E) = \sqrt{\frac{fN(4E^2 + M_A^2 N^2)}{2E^2 M_A}} \sqrt{\sqrt{4E^2 + M_A^2 N^2} - M_A N}. \quad (3.66)$$

As an example, let us consider the Schwarzschild solution, $N^2 = f = 1 - r_g/r$, for which we find

$$H = 2\sqrt{\frac{E}{M_A r_g^{3/2}}} (r - r_g)^{3/4} + \mathcal{O}((r - r_g)^{5/4}),$$

as $r \rightarrow r_g$, so that t remains finite. On the other hand, as $M_A \rightarrow \infty$,

⁵In the limit $M_A \rightarrow \infty$, this equation reduces to $\zeta - \frac{E^2}{N^2} = 0$, which is again consistent with the case $F(\zeta) = \zeta$.

⁶In the limit $M_A \rightarrow \infty$, this equation becomes $\frac{i^2}{\dot{i}^2} = fN^2$, which is again consistent with the case $F(\zeta) = \zeta$.

$$H = \frac{r - r_g}{r_g} + \frac{3E^2}{2M_A^2} + \mathcal{O}\left(\frac{1}{M_A^4}\right).$$

Thus, if we take the limit $M_A \rightarrow \infty$ before letting the trajectory approach r_g , then t will blow up logarithmically as $r \rightarrow r_g$. As a result, a horizon exists in this limit.

More generally, if f has an a th order zero and N^2 has a b th order zero at $r = r_g$, as given in Eq. (3.14), then we find that

$$H = 2\sqrt{\frac{E f_0(r_g) N_0(r_g)}{M_A}} (r - r_g)^{(a/2)+(b/4)} + \mathcal{O}((r - r_g)^{(a/2)+(3b/4)}),$$

as $r \rightarrow r_g$. It follows that

$$t \simeq t_0 + \frac{1}{2\sqrt{\frac{E f_0(r_g) N_0(r_g)}{M_A}}} \begin{cases} \frac{(r - r_g)^{1-(a/2)-(b/4)}}{1 - \frac{a}{2} - \frac{b}{4}} & \frac{a}{2} + \frac{b}{4} \neq 1 \\ \ln(r - r_g) & \frac{a}{2} + \frac{b}{4} = 1. \end{cases} \quad (3.67)$$

Therefore, t blows up as $r \rightarrow r_g$, if and only if

$$a + \frac{b}{2} \geq 2, \quad (3.68)$$

which is exactly Eq. (3.26) for $n = 2$, as expected.

IV. VACUUM SOLUTIONS WITH $N^r = 0$

When $N^r = 0$, the vacuum equations with $J^t = v = p_r = p_\theta = J_A = J_\varphi = 0$ yield the following most general solutions [41],

$$f(r) = 1 + \frac{C}{r} - \frac{1}{3} \Lambda_g r^2, \quad N = 1, \quad N^r = 0 = \varphi, \quad (4.1)$$

with the Hamiltonian constraint

$$\int \mathcal{L}_V e^\nu r^2 dr = 0, \quad (4.2)$$

where $\mathcal{L}_V = \mathcal{L}_V(r, \Lambda_g, C, g_s)$, as defined in Eq. (2.4).

The gauge field A must satisfy the equations

$$A' + A\nu' + \frac{1}{2} r F_{rr} = 0, \quad (4.3)$$

$$r^2(A'' - \nu'A') + r(A' + \nu'A) - A(1 - e^{2\nu}) + e^{2\nu} F_{\theta\theta} = 0, \quad (4.4)$$

where F_{ij} is given by Eqs. (2.12) and (A2). Then, from Eq. (4.3) we find that

$$A = A_0 e^{-\nu} - \frac{1}{2} e^{-\nu} \int^r r' e^{\nu(r')} F_{rr}(r') dr', \quad (4.5)$$

where A_0 is an integration constant. The solutions with $\Lambda_g = 0$ were first studied in [22,40].

Since now we have $N = 1$ and $b = 0$, Eq. (3.26) shows that a horizon exists only when $a \geq 2$. It can be shown that for the solutions given by Eq. (4.1), this is impossible for any chosen C and Λ_g . Therefore, it is concluded that the solutions given by Eq. (4.1) do not represent black holes.

However, in some cases $f(r) = 0$ does have a real and positive root. So, there indeed exists some kind of coordinate singularities, and to obtain a maximally (geodesically) complete spacetime,⁷ some kind of extension is needed. Such an extension is also needed in order to determine the range of r , from which the Hamiltonian constraint (4.2) can be carried out. Once this constraint is satisfied, one can integrate Eq. (4.5) to obtain the gauge field A . To this end, we divide the solutions into the following cases: (i) $C = \Lambda_g = 0$, (ii) $C \neq 0$, $\Lambda_g \neq 0$, (iii) $C \neq 0$, $\Lambda_g = 0$, and (iv) $C \neq 0$, $\Lambda_g \neq 0$. The first case is trivial, and it corresponds to the Minkowski spacetime with $\nu = \Lambda = 0$ and $A = A_0$. Thus, in the following we shall consider only the last three cases.

A. $C \neq 0, \Lambda_g = 0$

In this case the metric takes the form

$$ds^2 = -dt^2 + \frac{dr^2}{1 + \frac{C}{r}} + r^2 d^2\Omega, \quad (4.6)$$

from which we find that

$$\mathcal{L}_V = 2\Lambda + \frac{3g_3 C^2}{2\zeta^2 r^6} + \frac{3g_6 C^3}{4\zeta^4 r^9} + \frac{45g_8 C^2}{2\zeta^4 r^8} \left(1 + \frac{C}{r}\right), \quad (4.7)$$

where $\Lambda = g_0 \zeta^2 / 2$. To consider the Hamiltonian constraint (4.2), we need to further distinguish the cases $C > 0$ and $C < 0$.

I. $C > 0$

When $C > 0$, the metric (4.6) is singular only at $r = 0$, so the solution covers the whole spacetime $r \in (0, \infty)$. The singularity at the center is a curvature one [46], as it can be seen from the expressions

$$\begin{aligned} R^{ij}R_{ij} &= \frac{3C^2}{2r^6}, \\ R^i{}_j R^j{}_k R^k{}_i &= -\frac{3C^3}{4r^9}, \\ (\nabla_i R_{jk})(\nabla^i R^{jk}) &= \frac{45C^2}{2r^8} \left(1 + \frac{C}{r}\right). \end{aligned} \quad (4.8)$$

Since event horizons do not exist for $C > 0$, this singularity is also naked. Inserting it into Eq. (4.2), we find that the Hamiltonian constraint is satisfied only when

⁷Because of the breaking of the general covariance and the restricted diffeomorphism (1.2), it is not clear if this requirement is still applicable here in the HL theory. Even if it is not, some kind of extension still seems needed.

$$\Lambda = g_3 = g_6 = g_8 = 0. \quad (4.9)$$

Considering Eq. (A2), we find that F_{ij} now has only two nonvanishing terms, given by

$$F_{ij} = -(F_1)_{ij} + \frac{g_5}{\zeta^4} (F_5)_{ij}. \quad (4.10)$$

Substituting this into Eqs. (4.3) and (4.4), we obtain

$$A = 1 + A_0 \sqrt{1 + \frac{C}{r}}, \quad g_5 = 0. \quad (4.11)$$

It should be noted that the above solution holds not only in the IR regime but also in the UV.

To study the global structure of the spacetime, let us first introduce a new radial coordinate r^* via the relation

$$\begin{aligned} r^* &\equiv \int \frac{dr}{\sqrt{1 + \frac{C}{r}}} = -\frac{C}{2} \ln \frac{(\sqrt{r+C} + \sqrt{r})^2}{C} + \sqrt{r(r+C)} \\ &= \begin{cases} 0 & r = 0 \\ \infty & r = \infty. \end{cases} \end{aligned} \quad (4.12)$$

In terms of r^* the metric takes the form

$$ds^2 = -dt^2 + dr^{*2} + r^2(r^*)d^2\Omega. \quad (4.13)$$

Then, one might introduce the two double null coordinates u and v via the relations

$$u = \tan^{-1}(t + r^*), \quad v = \tan^{-1}(t - r^*), \quad (4.14)$$

so that the metric finally takes the form

$$ds^2 = -\frac{dudv}{\cos^2 u \cos^2 v} + r^2(u, v)d^2\Omega, \quad (4.15)$$

where $-\pi/2 \leq u, v \leq \pi/2$. The corresponding Penrose diagram is given by Fig. 2.

However, the coordinate transformations (4.14) are not allowed by the foliation-preserving diffeomorphisms $\text{Diff}(M, \mathcal{F})$ of Eq. (1.2). So, in the HL theory the restricted diffeomorphisms do not permit Penrose diagrams. In addition, due to the breaking of the general covariance, even if one were allowed to do so, the causal structure of the spacetime cannot be studied in terms of it, as shown explicitly in the previous sections for the Newtonian theory.

The following coordinate transformations are allowed,

$$t = \tan \bar{t}, \quad r^* = \tan \bar{r}^*, \quad (4.16)$$

where $-\pi/2 \leq \bar{t} \leq \pi/2$ and $0 \leq \bar{r}^* \leq \pi/2$. Then, the global structure of the spacetime is given by Fig. 3.

2. $C < 0$

In this case, setting $C = -2M < 0$, the corresponding metric reads

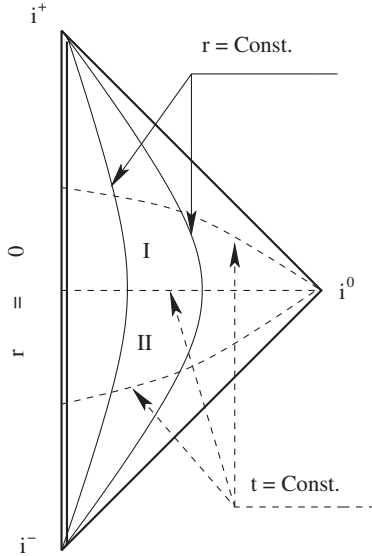


FIG. 2. The Penrose diagram for $N^r = 0$, $C > 0$, and $\Lambda_g = 0$. The double vertical solid lines represent the center ($r = 0$), at which the spacetime is singular. This singularity is clearly naked. Note that the restricted diffeomorphisms (1.2) do not allow for the transformations needed in order to draw Penrose diagrams. Therefore, these diagrams cannot be used to study the global structures of spacetimes in the HL theory but are included only for comparison.

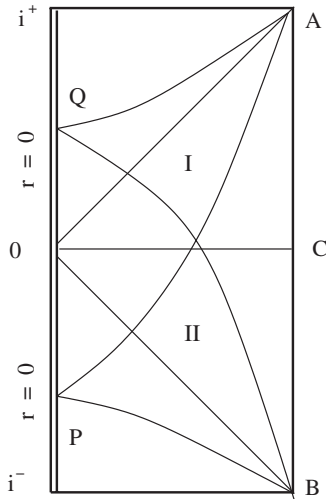


FIG. 3. The global structure of the spacetime in the (\tilde{t}, \tilde{r}^*) plane for $N^r = 0$, $C > 0$, and $\Lambda_g = 0$. The double vertical solid lines represent the center ($r = 0$), at which the spacetime is singular. The vertical line AB represents the spatial infinity $r = \infty$, while the horizontal line $i^+A(i^-B)$ is the line where $t = \infty$ ($t = -\infty$). The lines $t = \text{Const}$ are the straight lines parallel to OC , while the ones $r = \text{Const}$ are the straight lines parallel to i^-i^+ . The lines BP , $B0$, BQ , PA , $0A$, and QA represent the radial null geodesics.

$$ds^2 = -dt^2 + \left(1 - \frac{2M}{r}\right)^{-1} dr^2 + r^2 d^2\Omega. \quad (4.17)$$

This is the solution first found in [22], in which it was argued that the relativistic lapse function should be $\mathcal{N} = N - A$ in the IR. It is not clear how to then relate \mathcal{N} to N and A in other regimes. Instead, in this paper we shall simply take the point of view that A and φ are just gravitational gauge fields, and their effects on the spacetime itself occur only through the field equations [41]. With the above arguments, we can consider the solution valid in any regimes, including the IR and UV.

Let us first note that the metric (4.6) is asymptotically flat and singular at both $r = 0$ and $r = 2M$. The singularity at $r = 0$ is a curvature one, as can be seen from Eq. (4.8), but the one at $r = 2M$ is more peculiar. In particular, in the region $r < 2M$ both t and r are timelike, in contrast to GR where t and r exchange their roles across $r = 2M$. All the above indicate that the nature of the singularity at $r = 2M$ is now different. In fact, as to be shown explicitly below, the region $r < 2M$ is actually not part of the spacetime.

To see this closely, let us first consider the radial timelike geodesics. It can be shown that they are given by

$$\begin{aligned} t &= E\tau + t_0, \\ \tau &= \pm \frac{1}{\sqrt{E^2 - 1}} \{M \ln[(r - M) + \sqrt{r(r - 2M)}] \\ &\quad - \sqrt{r(r - 2M)}\} + \tau_0, \end{aligned} \quad (4.18)$$

where E is an integration constant, and τ denotes the proper time. The constant τ_0 is chosen so that $\tau(r_0) = 0$ at the initial position of the test particle, $r = r_0 > 2M$. The “+” (“-”) sign corresponds to the outgoing (ingoing) radial geodesics. It is clear that, starting at any given finite radius r_0 , observers that follow the null geodesics will arrive at $r = 2M$ within a finite proper time.⁸ Setting

$$e_{(0)}^\alpha \equiv \frac{dx^\alpha}{d\tau} = \left(E, -\sqrt{(E^2 - 1)}f, 0, 0\right), \quad (4.19)$$

where $f \equiv 1 - 2M/r$, we find that the spacelike unit vectors

$$\begin{aligned} e_{(1)}^\alpha &= (\sqrt{E^2 - 1}, -E\sqrt{f}, 0, 0), \\ e_{(2)}^\alpha &= \frac{1}{r}(0, 0, 1, 0), \\ e_{(3)}^\alpha &= \frac{1}{r \sin\theta}(0, 0, 0, 1), \end{aligned} \quad (4.20)$$

together with $e_{(0)}^\alpha$, form a freely falling frame,

⁸As shown in the last section, massless test particles in the HL theory do not follow null geodesics, because of the nonrelativistic dispersion relations (1.5). In other words, in the HL theory particles that follow the null geodesics are not massless and may not even be test particles.

$$e_{(a)}^\alpha e_{\alpha(b)} = \eta_{ab}, \quad e_{(0)}^\alpha D_\alpha e_{(a)}^\beta = 0, \quad (4.21)$$

where D_α denotes the 4D covariant derivatives, and η_{ab} is the 4D Minkowski metric with $a, b, = 0, \dots, 3$. Then, from the geodesic deviations,

$$\frac{D^2 \eta^a}{D\tau^2} + \mathcal{K}_b^a \eta^b = 0, \quad (4.22)$$

where $\mathcal{K}_{ab} \equiv -R_{\sigma\alpha\beta\gamma} e_{(a)}^\sigma e_{(0)}^\alpha e_{(0)}^\beta e_{(b)}^\gamma$ denotes the tidal forces exerted on the observers, we find that in the present case \mathcal{K}_{ab} is given by

$$\mathcal{K}_{ab} = -\frac{(E^2 - 1)M}{r^3} (\delta_a^2 \delta_b^2 + \delta_a^3 \delta_b^3). \quad (4.23)$$

Clearly, \mathcal{K}_{ab} is finite at $r = 2M$. All the above considerations indicate that the singularity at $r = 2M$ is a coordinate one, and to have a (geodesically) complete spacetime, extension beyond this surface is needed. However, unlike that in GR, any extension must be restricted to the $\text{Diff}(M, \mathcal{F})$ of Eq. (1.2). Otherwise, the resulting solutions do not satisfy the field equations. Explicit examples of this kind were given in [46].

In [22], the isotropic coordinate ρ was introduced,

$$r = \rho \left(1 + \frac{M}{2\rho}\right)^2, \quad (4.24)$$

in terms of which the metric (4.6) takes the form

$$ds^2 = -dt^2 + \left(1 + \frac{M}{2\rho}\right)^4 (d\rho^2 + \rho^2 d^2\Omega), \quad (4.25)$$

which is nonsingular for $\rho > 0$. However, this cannot be considered as an extension to the region $r < 2M$, as now the geometrical radius r is still restricted to $r \in (2M, \infty)$ for $\rho > 0$, as shown by curve (a) in Fig. 4. Instead, it connects two asymptotic regions, where $r = 2M$ acts as a throat, a situation quite similar to the Einstein-Rosen bridge [47]. However, a fundamental difference of the metric (4.25) from the corresponding one in GR is that it is not singular for any $\rho \in (0, \infty)$, while in GR the metric

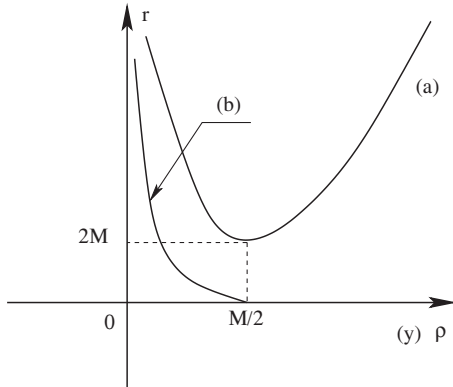


FIG. 4. The function r defined in (a) by Eq. (4.24) and in (b) by Eq. (4.31).

still has a coordinate singularity at $\rho = M/2$ (or $r = 2M$) [47]. Therefore, in the HL theory Eq. (4.25) already represents an extension of the metric (4.6) beyond the surface $r = 2M$. Since this extension is analytical, it is unique. It is remarkable to note that in this extension the metric has the correct signature.

It should be noted that the Einstein-Rosen bridge is not stable in GR [47]. Therefore, it would be very interesting to know if this is still the case in the HL theory.

To study its global structure, we introduce the coordinate r^* by

$$r^* \equiv \int \left(1 + \frac{M}{2\rho}\right)^2 d\rho = M \ln\left(\frac{2\rho}{M}\right) + \rho \left(1 - \frac{M^2}{4\rho^2}\right) \\ = \begin{cases} -\infty & \rho = 0 \\ \infty & \rho = \infty. \end{cases} \quad (4.26)$$

Then, in terms of r^* the metric can also be cast in the form of Eq. (4.13). Following what was done in that case, one can see that the global structure of the spacetime is given by Fig. 5.

To compare it with that given in GR, the corresponding Penrose diagram is presented in Fig. 6, although it is forbidden in the HL theory by the foliation-preserving diffeomorphisms $\text{Diff}(M, \mathcal{F})$ of Eq. (1.2), as mentioned above.

It is interesting to see which kind of matter fields can give rise to such a spacetime in GR. To this purpose, we

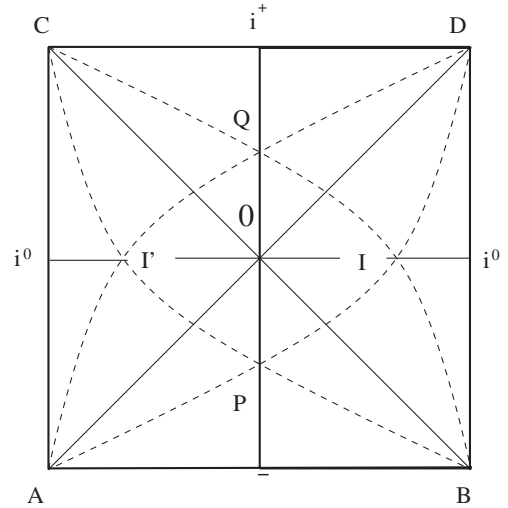


FIG. 5. The global structure of the spacetime for $N^r = 0$, $C = -2M < 0$, and $\Lambda_g = 0$. The vertical line $i^+ i^-$ represents the Einstein-Rosen throat ($r = r_g \equiv 2M$), which is nonsingular and connects the two asymptotically flat regions I and I' . The horizontal line $AB(CD)$ is the line where $t = -\infty(\infty)$, while the vertical lines CA and DB are the lines where $r = \infty$. The lines $t = \text{Const}$ are the straight lines parallel to $i^0 i^0$, while the ones $r = \text{Const}$ are the straight lines parallel to $i^- i^+$. The curved dotted lines AD and BC , as well as the straight solid lines AD and BC , are the radial null geodesics.

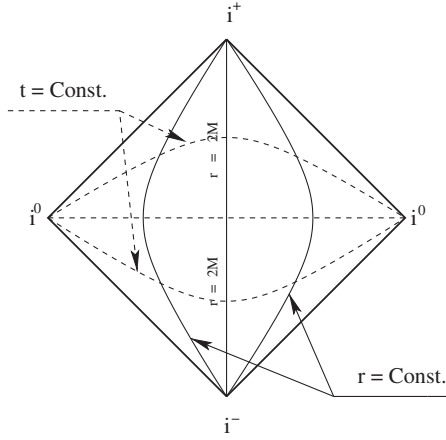


FIG. 6. The Penrose diagram for $N^r = 0$, $C = -2M < 0$, and $\Lambda_g = 0$. The straight lines i^+i^0 represent the future null infinities at which we have $r = \infty$ and $t = \infty$, while the ones i^-i^0 represent the past null infinities where $r = \infty$ and $t = -\infty$. The vertical line i^+i^- represents the Einstein-Rosen throat ($r = 2M$), which is nonsingular and connects the two asymptotically flat regions.

first calculate the corresponding four-dimensional Einstein tensor,

$${}^{(4)}G_{\mu\nu} = \frac{2M}{r^3 f} \delta_\mu^r \delta_\nu^r - \frac{M}{r} (\delta_\mu^\theta \delta_\nu^\theta + \sin^2 \theta \delta_\mu^\phi \delta_\nu^\phi), \quad (4.27)$$

which corresponds to an anisotropic fluid, $T_{\mu\nu}^{\text{GR}} = \rho^{\text{GR}} u_\mu u_\nu + p_r^{\text{GR}} r_\mu r_\nu + p_\theta^{\text{GR}} (\delta_\mu^\theta \delta_\nu^\theta + \sin^2 \theta \delta_\mu^\phi \delta_\nu^\phi)$, with $\rho^{\text{GR}} = 0$, $p_r^{\text{GR}} = M/(4\pi \text{GR}^3)$ and $p_\theta^{\text{GR}} = -Mr/(8\pi G)$, where $u_\mu = \delta_\mu^t$ and $r_\mu = f^{-1/2} \delta_\mu^r$. Clearly, such a fluid does not satisfy any of the energy conditions [32]. In particular, when $r \gg 1$ the tangential pressure becomes unbounded from below, while the radial pressure vanishes. Such a fluid is usually considered as nonphysical in GR. However, in the current setup the spacetime is vacuum, and one cannot eliminate it by simply considering the energy conditions. Then, if the configuration is stable, one can use it to construct time machines [48].

Inserting Eq. (4.7) into Eq. (4.2), and considering the fact that the range of r is now $r \in (2M, \infty)$, we find that the Hamiltonian constraint is satisfied, provided that

$$\Lambda = 0, \quad 20(g_6 - 3g_8) - 231g_3 \zeta^2 M^2 = 0. \quad (4.28)$$

Then, Eqs. (4.3) and (4.4) have the solution

$$A = 1 + A_0 \sqrt{1 - \frac{2M}{r}} + \frac{g_3}{40\zeta^2 M^2 r^6} [16(r - M)r^5 - 8M^2(r + M)r^3 - 3M^3(5r^2 + 7Mr + 1050M^2)],$$

$$g_5 = g_8 = 0. \quad (4.29)$$

It is interesting to note that, replacing ρ by $-y$ we find that, in terms of y , metric (4.25) takes the form

$$ds^2 = -dt^2 + \left(1 - \frac{M}{2y}\right)^4 (dy^2 + y^2 d^2\Omega), \quad (4.30)$$

from which we can see that the geometrical radius is now given by

$$r = y \left(1 - \frac{M}{2y}\right)^2. \quad (4.31)$$

Clearly, the whole region $0 \leq r < \infty$ is now mapped to $0 < y \leq M/2$, as shown by curve (b) in Fig. 4. Metric (4.30) can also be obtained from metric (4.25) by the replacement $M \rightarrow -M$ and $\rho \rightarrow y$. So, it must correspond to the case $C > 0$, i.e., the one with a negative mass, described in the previous subcase.

B. $C = 0$, $\Lambda_g \neq 0$

We have

$$\nu = -\frac{1}{2} \ln(1 - \frac{1}{3}\Lambda_g r^2), \quad (4.32)$$

for which we find that

$$\begin{aligned} \mathcal{L}_V &= 2(\Lambda - \Lambda_g) + \frac{4(3g_2 + g_3)}{3\zeta^2} \Lambda_g^2 \\ &\quad + \frac{8(9g_4 + 3g_5 + g_6)}{9\zeta^4} \Lambda_g^3, \\ F_{ij} &= \frac{g_{ij}}{9\zeta^4} [3\zeta^4(\Lambda_g - 3\Lambda) + 2\zeta^2(3g_2 + g_3)\Lambda_g^2 \\ &\quad + 4(9g_4 + 3g_5 + g_6)\Lambda_g^3]. \end{aligned} \quad (4.33)$$

To study the solutions further, we consider the cases $\Lambda_g > 0$ and $\Lambda_g < 0$, separately.

1. $\Lambda_g < 0$

In this case, defining $r_g \equiv \sqrt{3/|\Lambda_g|}$, we find that the corresponding metric takes the form

$$ds^2 = -dt^2 + \frac{dr^2}{1 + \left(\frac{r}{r_g}\right)^2} + r^2 d^2\Omega, \quad (4.34)$$

which shows that the metric is not singular except at $r = 0$. But, it can be shown that this is a coordinate singularity. Setting

$$r^* \equiv \int \frac{dr}{\sqrt{1 + \left(\frac{r}{r_g}\right)^2}} = r_g \ln \left[\frac{r}{r_g} + \sqrt{1 + \left(\frac{r}{r_g}\right)^2} \right], \quad (4.35)$$

one can cast the metric (4.34) exactly in the form of Eq. (4.13). Then, its global structure is that of Fig. 3, and the corresponding Penrose diagram is given by Fig. 2, but now the center $r = 0$ is free of any spacetime singularity. Thus, the range of r is now $r \in [0, \infty)$. We then find that

the Hamiltonian constraint (4.2) is satisfied, provided that $\mathcal{L}_V = 0$, i.e.,

$$\begin{aligned} & \Lambda \zeta^4 r_g^6 + 6(3g_2 + g_3)\zeta^2 r_g^2 - 12(9g_4 + 3g_5 + g_6) \\ & = -3\zeta^4 r_g^4. \end{aligned} \quad (4.36)$$

Inserting the above into Eqs. (4.3) and (4.4), we obtain the solution

$$A = A_0 \sqrt{1 + \left(\frac{r}{r_g}\right)^2} + A_1, \quad (4.37)$$

where A_1 is a constant, given by

$$A_1 \equiv 1 - \Lambda r_g^2 - \frac{3 - 3g_2 - g_3}{\zeta^2 r_g^2}. \quad (4.38)$$

2. $\Lambda_g > 0$

In this case, the corresponding metric takes the form

$$ds^2 = -dt^2 + \frac{dr^2}{1 - \left(\frac{r}{r_g}\right)^2} + r^2 d^2\Omega. \quad (4.39)$$

Clearly, the metric has a wrong signature in the region $r > r_g$. In fact, the hypersurface $r = r_g$ already represents the geometrical boundary of the spacetime, and any extension beyond it is not needed. To see this clearly, we first introduce the coordinate r^* via the relation

$$r^* \equiv \int \frac{dr}{\sqrt{1 - \left(\frac{r}{r_g}\right)^2}} = r_g \arcsin\left(\frac{r}{r_g}\right). \quad (4.40)$$

Then, in terms of r^* the corresponding metric can be cast in the form $ds^2 = r_g^2 d\bar{s}^2$, where

$$d\bar{s}^2 = -d\bar{t}^2 + dx^2 + \sin^2 x d^2\Omega, \quad (4.41)$$

with $\bar{t} = t/r_g$, $x = r^*/r_g$. But, this is exactly the homogeneous and isotropic Einstein static universe, which is geodesically complete for $-\infty < \bar{t} < \infty$, $0 \leq x \leq \pi$, $0 \leq \theta \leq \pi$, and $0 \leq \phi \leq 2\pi$, with an $R \times S^3$ topology [32]. Then, it is easy to see that its global structure is given by Fig. 3, but now the vertical line $i^- i^+$ is free of spacetime singularity, and the line AB is the one where $r = r_g$ (or $x = \pi$). The corresponding Penrose diagram is given by Fig. 7.

Therefore, in this case the range of r is $r \in [0, r_g]$. Then, the Hamiltonian constraint (4.2) requires

$$\Lambda \zeta^4 r_g^6 + 6(3g_2 + g_3)\zeta^2 r_g^2 + 12(9g_4 + 3g_5 + g_6) = 3\zeta^4 r_g^4. \quad (4.42)$$

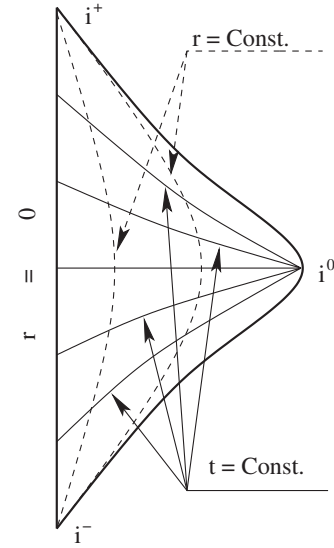


FIG. 7. The Penrose diagram for $N^r = 0$, $C = 0$, and $\Lambda_g > 0$, which is the Einstein static universe. The curves $i^- i^0$ and $i^+ i^0$ are, respectively, the lines where $t = -\infty$, $x = \pi$, and $t = +\infty$, $x = \pi$.

Hence, Eqs. (4.3) and (4.4) have the solution

$$A = A_0 \sqrt{1 - \left(\frac{r}{r_g}\right)^2} + A_2, \quad (4.43)$$

where A_2 is another integration constant, given by

$$A_2 \equiv 1 + \Lambda r_g^2 + \frac{3 - 3g_2 - g_3}{\zeta^2 r_g^2}. \quad (4.44)$$

It should be noted that in GR the Einstein static universe is obtained by the exact balance between the gravitational attraction of matter ($\rho_m = \rho_c$, $p_m = 0$) and the cosmic repulsion ($\Lambda = \Lambda_c$), where $\Lambda_c = 4\pi G\rho_c$. As a result, the configuration is not stable against small perturbations [49]. However, in the present case since the spacetime is vacuum, Eq. (4.42) suggests that the balance is made by the attraction of the high-order curvature derivatives and the cosmic repulsion, produced by both Λ and Λ_g . Then, it would be very interesting to know whether it is stable or not in the current setup.

C. $C \neq 0$, $\Lambda_g = 0$

When $\Lambda_g C \neq 0$, we find that

$$\begin{aligned} R^{ij}R_{ij} &= \frac{9C^2 + 8\Lambda_g^2 r^6}{6r^6}, \\ R_j^i R_k^j R_i^k &= \frac{1}{36r^9} (27C^3 + 108\Lambda_g C^2 r^3 + 32\Lambda_g^3 r^9), \\ (\nabla_i R_{jk})(\nabla^i R^{jk}) &= \frac{45C^2}{2r^8} \left(1 + \frac{C}{r} - \frac{1}{3}\Lambda_g r^2\right). \end{aligned} \quad (4.45)$$

from which one can see that the spacetime is singular at $r = 0$. Moreover, we find from (A2) that

$$\begin{aligned}
 F_{rr} = & \frac{1}{36r^8\zeta^4 F(r)} \{-27C^3(22g_5 + 25g_6 - 20g_8) \\
 & - 81C^2r(8g_5 + 9g_6 - 7g_8) \\
 & - 9C^2r^3[\Lambda_g(-26g_5 - 30g_6 + 25g_8) + \zeta^2g_3] \\
 & + 12Cr^6[-3\zeta^4 + \Lambda_g\zeta^2(12g_2 + 5g_3) \\
 & + \Lambda_g^2(36g_4 + 14g_5 + 6g_6 - g_8)] \\
 & + 4r^9[-3\zeta^4(3\Lambda - \Lambda_g) + 2\zeta^2\Lambda_g^2(3g_2 + g_3) \\
 & + 4\Lambda_g^3(9g_4 + 3g_5 + g_6)]\}, \quad (4.46)
 \end{aligned}$$

where the third-order polynomial $F(r)$ is defined by

$$F(r) = C + r - \frac{\Lambda_g}{3}r^3, \text{ i.e. } e^{2\nu} = \frac{r}{F(r)}.$$

The function \mathcal{L}_V is given by

$$\mathcal{L}_V = \frac{\alpha + \beta r + \gamma r^3 + \delta r^9}{36r^9\zeta^4}, \quad (4.47)$$

where

$$\begin{aligned}
 \alpha &= 27C^3g_6 + 810C^3g_8, \\
 \beta &= 810C^2g_8, \\
 \gamma &= 108C^2g_5\Lambda_g + 108C^2g_6\Lambda_g - 270C^2g_8\Lambda_g + 54C^2g_3\zeta^2, \\
 \delta &= 144g_2\zeta^2\Lambda_g^2 + 288g_4\Lambda_g^3 + 96g_5\Lambda_g^3 + 32g_6\Lambda_g^3 \\
 &+ 48g_3\zeta^2\Lambda_g^2 + 72\zeta^4\Lambda - 72\zeta^4\Lambda_g.
 \end{aligned}$$

All the quantities in (4.45) are finite for any $r \neq 0$. On the other hand, from Eq. (4.1) one can see that the metric coefficient g_{rr} could become singular at some points. To study the nature of these singularities, we distinguish the four cases: $C > 0, \Lambda_g > 0$; $C > 0, \Lambda_g < 0$; $C < 0, \Lambda_g > 0$; and $C < 0, \Lambda_g < 0$.

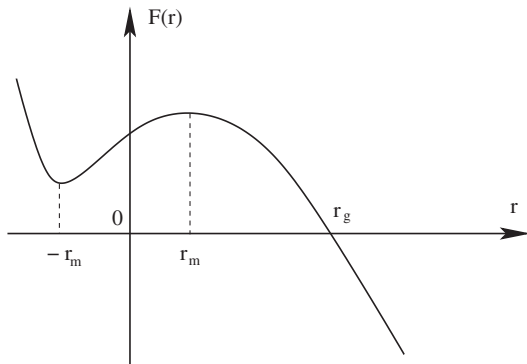


FIG. 8. The function $F(r) \equiv re^{-2\nu}$ for $N^r = 0, C > 0$, and $\Lambda_g > 0$, where $r_m = 1/\sqrt{\Lambda_g}$.

I. $C > 0, \Lambda_g > 0$

In this case, the polynomial $F(r)$ has exactly one real positive root at, say, $r = r_g(C, \Lambda_g) > 0$, as shown in Fig. 8. We find that

$$e^{2\nu} = \frac{r}{D(r)(r_g - r)}, \quad (4.48)$$

where $D(r) \equiv \Lambda_g(r^2 + r_g r + d)/3$, $d = r_g^2 - 3/\Lambda_g$, and $D(r) > 0$ for all $r > 0$. Introducing the coordinate x via the relation

$$x = \int \frac{dr}{2\sqrt{r_g - r}} = -\sqrt{r_g - r}, \quad (4.49)$$

or, inversely, $r = r_g - x^2$, the corresponding metric in terms of x takes the form

$$ds^2 = -dt^2 + \frac{4(r_g - x^2)}{D(x)}d^2x + (r_g - x^2)^2d^2\Omega, \quad (4.50)$$

where $D(x) = \Lambda_g(x^4 - 3r_g x^2 + 3r_g^2 - 3/\Lambda_g)/3 > 0$ for $|x| < \sqrt{r_g}$. Clearly, the coordinate singularity at $r = r_g$ (or $x = 0$) is now removed, and the metric is well defined for $|x| < \sqrt{r_g}$. At the points, $x = \pm\sqrt{r_g}$ (or $r = 0$), the spacetime is singular, as shown by Eq. (4.45). Thus, in the present case the spacetime is restricted to the region $|x| < \sqrt{r_g}$, $-\infty < t < \infty$ in the (t, x) plane, with the two spacetime singularities located at $x = \pm\sqrt{r_g}$ as its boundaries. The global structure of the spacetime and the corresponding Penrose diagram are shown in Fig. 9.

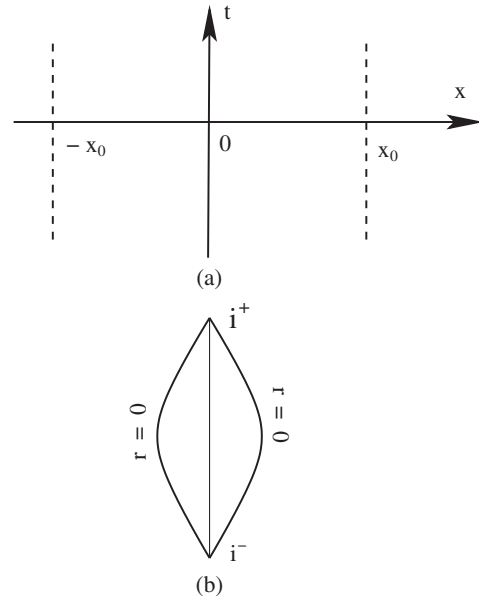


FIG. 9. (a) The spacetime in the (t, x) plane, where $x_0 \equiv \sqrt{r_g}$. (b) The Penrose diagram for $N^r = 0, C > 0, \Lambda_g > 0$. The curves i^-i^+ are the lines where $r = 0$, at which the spacetime is singular. The straight line i^-i^+ represents the surface $r = r_g$.

The change of variables (4.49) can be understood by considering the one-form

$$e^\nu dr = \frac{\sqrt{r} dr}{\sqrt{D(r)(r_g - r)}}.$$

Even though the denominator of the right-hand side vanishes at $r = r_g$, we can turn $e^\nu dr$ into a nonsingular one-form by introducing a Riemann surface. Indeed, if we promote r to a complex variable and define the genus 1 Riemann surface Σ as the two-sheeted cover of the complex r plane obtained by introducing two branch cuts along the intervals $[0, r_g]$ and $[r_1, r_2]$, where r_1 and r_2 are the two (possibly complex) zeros of $D(r)$, $e^\nu dr$ is a holomorphic one-form on Σ . Letting $(0, r_g]_1$ and $(0, r_g]_2$ denote the covers of the interval $(0, r_g]$ in the first and second sheets of Σ , respectively, the spacetime consists of points (r, θ, ϕ, t) with $r \in (0, r_g]_1 \cup (0, r_g]_2$. The variable $x = -\sqrt{r_g - r}$ introduced in (4.49) is analytic near the branch point at $r = r_g$, and $r \in (0, r_g]_1 \cup (0, r_g]_2$ corresponds to $x \in (-\sqrt{r_g}, \sqrt{r_g})$. We can fix the definition of x by choosing the branch of the square root so that, say, $x \geq 0$ for $r \in (0, r_g]_1$. Thus, in terms of the variable x , the spacetime manifold can be covered by a single global chart (no double cover is necessary), and the metric ds^2 , which involves the square of the differential $e^\nu dr$, is manifestly nonsingular at $r = r_g$. In particular, the metric of the extended spacetime is analytic, which ensures that the extension is unique.

The Hamiltonian constraint is

$$\int_0^{r_g} \mathcal{L}_V e^\nu r^2 dr = 0. \quad (4.51)$$

Indeed, the Hamiltonian constraint (2.5) should be interpreted as

$$\int \mathcal{L}_V \text{Vol}_g = 0, \quad (4.52)$$

where Vol_g is the volume form induced by the metric g_{ij} and the integration extends over a spatial slice of the spacetime. Using the variables (r, θ, ϕ) , we have

$$\text{Vol}_g = e^\nu r^2 \sin\theta dr d\theta d\phi,$$

and the integration extends over $\theta \in [0, \pi]$, $\phi \in [0, 2\pi]$, and $r \in [0, r_g]_1 \cup [0, r_g]_2$. By symmetry, the contributions from the sets where $r \in [0, r_g]_1$ and $r \in [0, r_g]_2$ are equal. Since each contribution is proportional to the left-hand side of (4.51), the constraint reduces to (4.51).

In view of (4.47), the constraint (4.51) becomes

$$\int_0^{r_g} \frac{\alpha + \beta r + \gamma r^3 + \delta r^9}{36r^7 \zeta^4 \sqrt{F(r)}} \sqrt{r} dr = 0. \quad (4.53)$$

Denoting the integrand in (4.53) by $I(r)$, we see that $|I(r)|$ is bounded by a constant times $1/\sqrt{r_g - r}$ as $r \rightarrow r_g$. Thus, the integral converges near r_g . On the other hand, as $r \rightarrow 0$,

$$I(r) = \frac{\alpha}{36r^{13/2} \zeta^4 \sqrt{C}} + O\left(\frac{1}{r^{11/2}}\right),$$

so that (4.53) can only be satisfied if $\alpha = 0$. Using similar arguments, we infer that the coefficients β, γ, δ must also vanish, i.e.,

$$\alpha = \beta = \gamma = \delta = 0.$$

Solving these equations, we conclude that the Hamiltonian constraint is satisfied if and only if the g_j 's satisfy the following four conditions:

$$\begin{aligned} g_4 &= \frac{\zeta^4(\Lambda_g - \Lambda) - 2g_2 \zeta^2 \Lambda_g^2}{4\Lambda_g^3}, \\ g_5 &= -\frac{g_3 \zeta^2}{2\Lambda_g}, \quad g_6 = 0, \quad g_8 = 0. \end{aligned} \quad (4.54)$$

Using the conditions (4.54) in the expression (4.46) for F_{rr} , we find that Eqs. (4.3) and (4.4) have the solution

$$A(r) = -\frac{\sqrt{F(r)}}{2\sqrt{r}} \int_{r_0}^r \frac{F_{rr}(r')(r')^{3/2} dr'}{\sqrt{F(r')}} \quad (4.55)$$

where

$$\begin{aligned} F_{rr} &= -\frac{1}{36r^8 \zeta^2 \Lambda_g F(r)} \{ -297C^3 g_3 - 324C^2 r g_3 \\ &\quad + 126C^2 r^3 \Lambda_g g_3 + 12Cr^6 [2\Lambda_g^2 (3g_2 + g_3) \\ &\quad + \zeta^2 (9\Lambda - 6\Lambda_g)] + 8r^9 \Lambda_g [2\Lambda_g^2 (3g_2 + g_3) \\ &\quad + \zeta^2 (9\Lambda - 6\Lambda_g)] \}, \end{aligned} \quad (4.56)$$

and $r_0 \in (0, r_g)$ is a constant. The integrand in (4.55) is smooth for $0 < r < r_g$. Thus, $A(r)$ is a smooth function of $r \in (0, r_g)$. Unless $g_3 = 0$, the integral diverges as $r \rightarrow 0$, so that $A(r)$ has a singularity at $r = 0$. As $r \rightarrow r_g$, the integrand is bounded by $\text{const} \times (r_g - r)^{-3/2}$. This implies that $A(r)$ is bounded as $r \rightarrow r_g$. In fact, viewed as a function on the Riemann surface Σ , $A(r)$ is analytic near $r = r_g$. This follows since the integrand in (4.55) is a meromorphic one-form with a pole of at most second order at $r = r_g$. Thus, the integral has a pole of at most order one at r_g , which is canceled by the simple zero of the prefactor $\sqrt{F(r)} = \sqrt{D(r)(r_g - r)}$. In conclusion, the gauge field A given by (4.55) is a smooth function everywhere on the extended spacetime away from the singularity at $r = 0$.

2. $C > 0, \Lambda_g < 0$

In this case, $F(r) > 0$ for $r > 0$ and the metric coefficient g_{rr} is positive and nonsingular except at the point $r = 0$, at which a naked spacetime singularity appears. The corresponding Penrose diagram is given by Fig. 2 with $r \in (0, \infty)$. The Hamiltonian constraint (4.2) requires that

$$\int_0^\infty \mathcal{L}_\nu e^\nu r^2 dr = 0. \quad (4.57)$$

As in the previous subsection, this constraint is equivalent to the conditions given in (4.54).

The function $A(r)$ is again given by the formulas (4.55) and (4.56) and is a smooth function of $r \in (0, \infty)$. As $r \rightarrow \infty$, the absolute value of the integrand is bounded by constant $\times r^{-2}$. Thus, choosing $r_0 = \infty$ in (4.55), we find that $A(r)$ is bounded as $r \rightarrow \infty$. Unless $g_3 = 0$, the integral diverges as $r \rightarrow 0$, so that $A(r)$ has a singularity at $r = 0$.

3. $C < 0, \Lambda_g > 0$

In this case, if $\Lambda_g > 4/(9C^2)$, $e^{2\nu} = r/F(r)$ is strictly negative for all $r > 0$, so that, in addition to t , the coordinate r is also timelike. The physics of such a spacetime is unclear, if there is any. Therefore, in the following we consider only the case

$$0 < \Lambda_g < \frac{4}{9C^2}. \quad (4.58)$$

Then, we find that $F(r)$ is positive only for $0 < r_- < r < r_+$, where $r_\pm(\Lambda_g, C)$ are the two positive roots of $F(r) = 0$, as shown in Fig. 10. We write $e^{2\nu}$ as

$$e^{2\nu} = \frac{r}{(r+r_0)(r-r_-)(r_+-r)}, \quad (4.59)$$

where $r_0(\Lambda_g, C) > 0$. To extend the solution beyond $r = r_\pm$, we shall first consider the extension beyond $r = r_-$. Such an extension can be obtained via

$$x = \int \frac{dr}{2\sqrt{r-r_-}} = \sqrt{r-r_-}, \quad (4.60)$$

or inversely, $r = x^2 + r_-$. Since $r < r_+$, we find that $-x_0 < x < x_0$ with $x_0 \equiv \sqrt{r_+ - r_-}$. It can be seen that the coordinate singularity at $r = r_-$ disappears, and the extended region is given by $|x| < x_0$, as shown by Fig. 11(a).

To extend the solution beyond r_+ , we introduce x via the relation

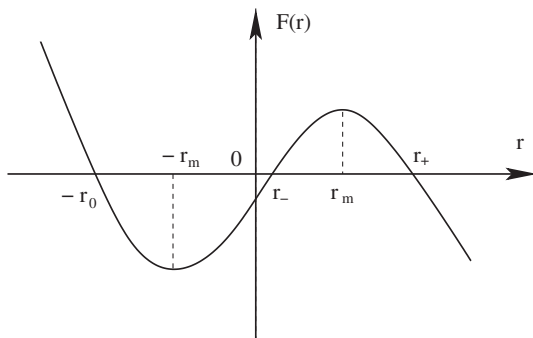


FIG. 10. The function $F(r) = re^{-2\nu}$ for $C < 0$ and $\Lambda_g > 0$, where $r_m \equiv 1/\sqrt{\Lambda_g}$. $F(r) = 0$ has two positive roots r_\pm only for $\Lambda_g < 4/(9C^2)$. When $\Lambda_g \geq 4/(9C^2)$, $F(r)$ is always nonpositive for any $r > 0$.

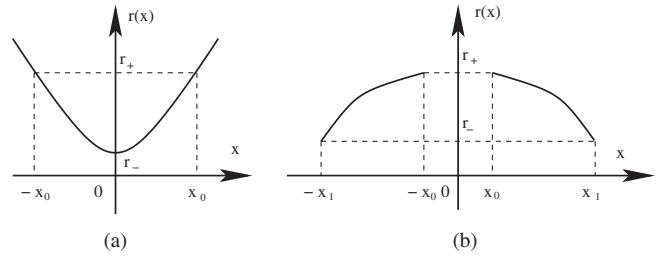


FIG. 11. (a) The function r vs x given by Eq. (4.60), where $x_0 \equiv \sqrt{r_+ - r_-}$. (b) The function r vs x given by Eq. (4.61), where $x_1 \equiv x_0 + \sqrt{x_0}$.

$$r = r_+ - (x \mp x_0)^2, \quad (4.61)$$

where the “ $-$ ” sign applies when $x > x_0$ and the “ $+$ ” sign applies when $x < -x_0$. Figure 11(b) shows the graph of r as a function of x . From Fig. 11 we can see that the extensions along both the positive and the negative directions of x need to continue in order to have a maximal spacetime. This can be done by repeating the above process infinitely many times, so finally the whole (t, x) plane is covered by an infinite number of finite strips, in each of which we have $r_- \leq r \leq r_+$. The global structure is that of Fig. 12, and the corresponding Penrose diagram is given by Fig. 13. Thus, in this case we have $r \in [r_-, r_+]$.

The Hamiltonian constraint (4.2) requires that

$$\int_{r_-}^{r_+} \frac{\alpha + \beta r + \gamma r^3 + \delta r^9}{36r^7 \zeta^4 \sqrt{F(r)}} \sqrt{r} dr = 0. \quad (4.62)$$

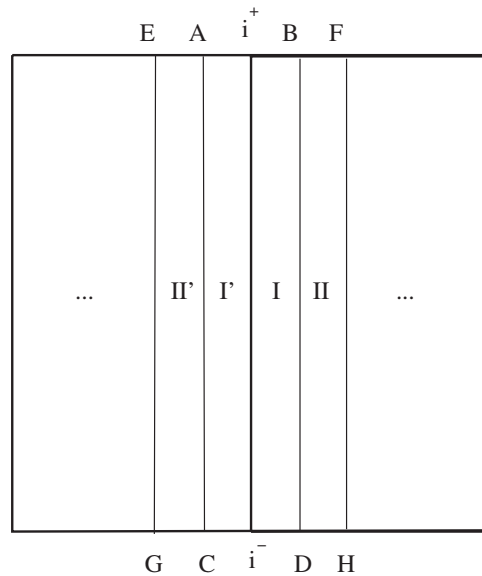


FIG. 12. The global structure of the spacetime for $C < 0$, $\Lambda_g > 0$, and $\Lambda_g < 4/(9C^2)$. The vertical line $i^+ i^-$ is the one where $r = r_-$, and the ones AC and BD represent the lines where $r = r_+$, while on the lines EG and FH we have $r = r_-$. The spacetime repeats itself infinitely many times in both directions of the x axis.

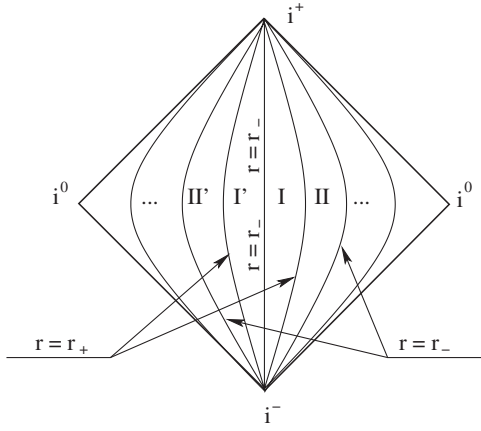


FIG. 13. The Penrose diagram for $C < 0$, $\Lambda_g > 0$, and $\Lambda_g < 4/(9C^2)$.

Geometrically, this condition can be understood by introducing a Riemann surface Σ as a double cover of the complex r plane with two branch cuts along $[r_-, r_+]$ and $[-r_0, 0]$. The integrand in (4.62) is a one-form ω on Σ which is holomorphic in the neighborhood of the closed curve $a_1 \equiv [r_-, r_+]_1 \cup [r_+, r_-]_2$. Topologically, the elliptic curve Σ is a torus, a_1 is a nontrivial cycle, and the condition (4.62) states that the integral of ω along the cycle a_1 vanishes. This imposes a constraint on the coefficients $\alpha, \beta, \gamma, \delta$, which translates into a condition on the g_j 's involving elliptic integrals. Assuming this condition holds, the function $A(r)$ is given by (4.55) with $r_0 \in (r_-, r_+)$ and F_{rr} as in (4.46).

4. $C < 0, \Lambda_g < 0$

In this case, the function $F(r) = re^{-2\nu}$ is positive only for $r > r_g$, as shown in Fig. 14. Thus, $e^{2\nu}$ can be written in the form

$$e^{2\nu} = \frac{r}{D(r)(r - r_g)}, \quad (4.63)$$

where $D(r) > 0$ for $r > 0$. The extension can be carried out by introducing a new coordinate x via the relation

$$r = x^2 + r_g. \quad (4.64)$$

In terms of x the coordinate singularity at $r = r_g$ disappears, and the extended spacetime is given by $-\infty < t, x < \infty$ in the (t, x) plane. Its global structure is given by Fig. 5, while the corresponding Penrose diagram is given by Fig. 6. Thus, in this case the range of r is $r \in [r_g, \infty)$.

The Hamiltonian constraint (4.2) requires that

$$\int_{r_g}^{\infty} \frac{\alpha + \beta r + \gamma r^3 + \delta r^9}{36r^7 \zeta^4 \sqrt{F(r)}} \sqrt{r} dr = 0.$$

The behavior of the integrand as $r \rightarrow \infty$ implies that

$$\alpha = \beta = \gamma = \delta = 0,$$

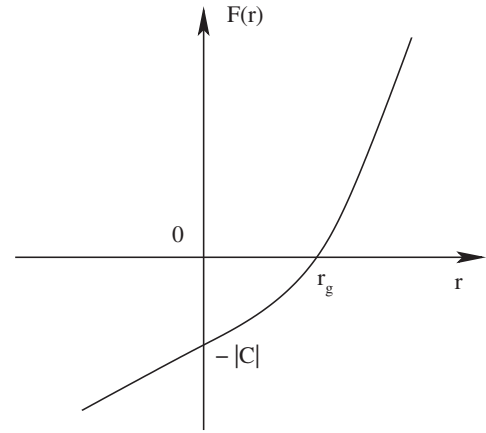


FIG. 14. The function $F(r) = re^{-2\nu}$ for $C < 0$ and $\Lambda_g < 0$, where r_g is the only positive root of $F(r) = 0$.

so that the constraint reduces to (4.54) and the function $A(r)$ is given by (4.55) and (4.56), which is not singular everywhere in the extended spacetime.

V. VACUUM SOLUTIONS WITH $N^r \neq 0$

When $N^r \neq 0$, the vacuum solutions are given by [41]

$$ds^2 = -dt^2 + e^{2\nu}(dr + e^{\mu-\nu}dt)^2 + r^2 d^2\Omega, \quad (5.1)$$

with

$$\mu = \frac{1}{2} \ln\left(\frac{2m}{r} + \frac{1}{3} \Lambda r^2 - 2A(r) + \frac{2}{r} \int^r A(r') dr'\right), \quad (5.2)$$

$$\nu = \varphi = \Lambda_g = 0,$$

where the gauge field A must satisfy the Hamiltonian constraint

$$\int_0^{\infty} r A'(r) dr = 0. \quad (5.3)$$

Otherwise, it is free. However, as shown in [41], the solar system tests seem to uniquely choose the Schwarzschild solution $A = 0$. Therefore, in the following we shall consider only this case,

$$\mu = \frac{1}{2} \ln\left(\frac{2m}{r} + \frac{1}{3} \Lambda r^2\right), \quad \nu = \varphi = \Lambda_g = A = 0. \quad (5.4)$$

It should be noted that if (N, ν, N^r) is a solution of the vacuum equations, so is $(N, \nu, -N^r)$. The latter can be easily obtained by the replacement $t \rightarrow -t$. With such changes, we have $K_{ij} \rightarrow -K_{ij}$ (in the static case). Clearly, these do not affect the singularity behavior. We then obtain [43,46]⁹

⁹There is a typo in the expression of K given by Eq. (3.2) in [46]. Although it propagates to other places, this does not affect our main conclusions, as K and $K_{ij}K^{ij}$ have similar singularity behavior.

$$R_{ij} = 0,$$

$$K = \epsilon_1 \sqrt{\frac{3}{r^3(6m + \Lambda r^3)}} (3m + \Lambda r^3), \quad (5.5)$$

$$K_{ij}K^{ij} = \frac{27m^2 + 6m\Lambda r^3 + \Lambda^2 r^6}{r^3(6m + \Lambda r^3)},$$

where $\epsilon_1 (= \pm 1)$ originates from the expression $N^r = \epsilon_1 e^\mu$, obtained by the replacement $t \rightarrow -t$, as mentioned above. To further study the above solutions, let us consider the following cases separately: (1) $m = 0, \Lambda = 0$; (2) $m = 0, \Lambda = 0$; and (3) $m = 0, \Lambda = 0$. We shall assume that $m \geq 0$, while Λ can take any value.

A. $m = 0, \Lambda \neq 0$

In this case, only $\Lambda > 0$ is allowed [41], as can be seen from Eq. (5.2). That implies that the anti-de Sitter spacetime cannot be written in the static form of Eq. (3.3) with the projectability condition. Then, we have $N^2 = f = 1$, $N^r = \epsilon_1 r/\ell$, or

$$ds^2 = -dt^2 + \left(dr + \epsilon_1 \frac{r}{\ell} dt \right)^2 + r^2 d^2\Omega, \quad (5.6)$$

where $\ell \equiv \sqrt{3/|\Lambda|}$. Without loss of generality, we shall consider only the case $\epsilon_1 = -1$, as the case $\epsilon_1 = 1$ can be simply obtained from the one $\epsilon_1 = -1$ by inverting the time coordinate. In terms of N, N^i, g_{ij} or their inverses, N_i, g^{ij} , the metric is nonsingular, except for the trivial $r = 0$ and $\theta = 0, \pi$. In addition, from Eq. (5.5) we also find that

$$K = -\sqrt{2\Lambda}, \quad K_{ij}K^{ij} = \Lambda, \quad (m = 0). \quad (5.7)$$

On the other hand, in terms of the four-dimensional metric, $g_{\mu\nu}$ and $g^{\mu\nu}$, it is not singular either, as one can see from the expressions

$$\begin{aligned} {}^{(4)}g_{\mu\nu} &= \begin{pmatrix} -\frac{\ell^2 - r^2}{\ell^2}, & -\frac{r}{\ell} \delta_i^r \\ -\frac{r}{\ell} \delta_r^i, & g_{ij} \end{pmatrix}, \\ {}^{(4)}g^{\mu\nu} &= \begin{pmatrix} -1, & -\frac{r}{\ell} \delta_r^i \\ -\frac{r}{\ell} \delta_r^i, & g^{ij} - \frac{r^2}{\ell^2} \delta_r^i \delta_r^j \end{pmatrix}, \end{aligned} \quad (5.8)$$

although the nature of the radial coordinate does change,

$$g^{\mu\nu} r_{,\mu} r_{,\nu} = 1 - \frac{r^2}{\ell^2} = \begin{cases} \text{timelike} & r > \ell \\ \text{null} & r = \ell \\ \text{spacelike} & r < \ell. \end{cases} \quad (5.9)$$

To study the solution further in the HL theory, we consider two different regimes, $E \ll M_*$ and $E \gg M_*$, where $M_* = \min\{M_A, M_B, \dots\}$ and M_n 's are the energy scales appearing in the dispersion relation (3.57).

I. $E \ll M_*$

When the energy E of the test particle is much less than M_* , from Eq. (3.57) one can see that $F(\zeta) \simeq \zeta$.

This corresponds to the relativistic case ($n = 1$), studied in Sec. III A 2. Then, for the ingoing test particles ($\epsilon = -1$), we have

$$H = N\sqrt{f} + N^r = \frac{\ell - r}{\ell}. \quad (5.10)$$

Thus, the hypersurface $r = \ell$ is indeed a horizon. In fact, it represents a cosmological horizon, as first found in GR [50].

However, because of the restricted diffeomorphisms (1.2), it is very interesting to see the global structure of the de Sitter spacetime in the HL theory. To this purpose, let us consider the coordinate transformations

$$t' = \ell e^{-t/\ell}, \quad r' = r e^{-t/\ell}, \quad (5.11)$$

in terms of which the corresponding metric takes the form

$$\begin{aligned} ds^2 &= -dt^2 + e^{2t/\ell} (dr'^2 + r'^2 d^2\Omega) \\ &= \left(\frac{\ell}{t'} \right)^2 (-dt'^2 + dr'^2 + r'^2 d^2\Omega). \end{aligned} \quad (5.12)$$

From Eq. (5.11) we can see that the whole (t, r) plane, $-\infty < t < \infty, r \geq 0$, is mapped to the region $t', r' \geq 0$. However, the metric now becomes singular at $t' = 0, \infty$ (or $t = \pm\infty$). To see the nature of these singularities, one may recall the five-dimensional embedding of the de Sitter spacetime in GR [32], from which we find that in terms of the five-dimensional coordinates v and w , t' is given by $t' = \ell^2/(v + w)$. Therefore, $t' \geq 0$ corresponds to $v + w \geq 0$. Thus, the region $t', r' \geq 0$ only represents the half hyperboloid $v + w \geq 0$, as shown by Fig. 16 (ii) in [32]. In particular, $t' = 0$ represents the boundary of the spacelike infinity, so extension beyond this surface may not be needed. Although the extension given in [32] in terms of the static Einstein universe coordinates $(\bar{t}, \bar{\chi}, \bar{\theta}, \bar{\phi})$ is forbidden here by the restricted diffeomorphisms (1.2), as that extension requires

$$t = \ell \ln \left[\cosh \left(\frac{\bar{t}}{\ell} \right) \cos(\bar{\chi}) + \sinh \left(\frac{\bar{t}}{\ell} \right) \right],$$

the extension across $t' = \infty$ (or $v + w = 0^+$) seems necessary.

Another way to see the need of an extension beyond $t' = 0$ is that the metric (5.12) is well defined for $t' < 0$. So, one may simply take $-\infty < t' < \infty$. But, this cannot be considered as an extension, as the metric (5.12) is singular at $t' = 0$, and the two regions $t' > 0$ and $t' < 0$ are not smoothly connected in the t', r' coordinates. In this sense, a proper extension is still needed. However, due to the restricted diffeomorphisms (1.2), it is not clear if such extensions exist or not. Figure 15 shows the global structure of the region $t' \geq 0$, which is quite different from its corresponding Penrose diagram [50].

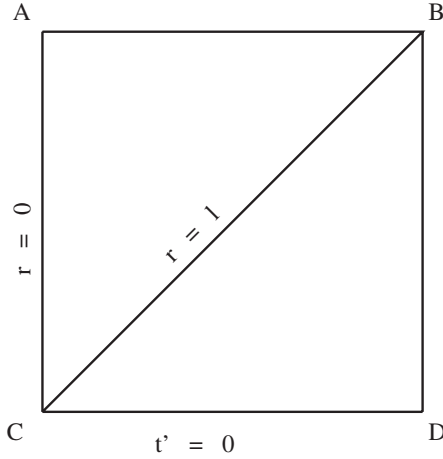


FIG. 15. The global structure of the de Sitter solution $N^2 = f = 1$, $N^r = -\sqrt{r}/\ell$ in the HL theory with the restricted diffeomorphisms (1.2) for the region $t' \geq 0$. The horizontal line AB corresponds to $t' = \infty$ (or $t = -\infty$), while the vertical line BD to $r' = \infty$ (or $r = \infty$).

2. $E \gg M_*$

When the energy E of the test particle is greater than M_* , from Eq. (3.57) one can see that high-order momentum terms become important, and $F(\zeta) \simeq \zeta^n$ ($n \geq 2$). For the sake of simplicity, we consider the case with $n = 2$ only. Then, from Eqs. (3.23) and (3.28) we find that

$$X = \frac{2\ell E}{\sqrt{r^2 + 4\ell^2 E} + r}, \quad H = \frac{r}{\ell} - \frac{4\ell E}{\sqrt{r^2 + 4\ell^2 E} + r}. \quad (5.13)$$

Thus, $H(r, E) = 0$ has only one real root,

$$r_H = \left(\frac{4\ell^2 E}{3}\right)^{1/2}, \quad (5.14)$$

at which we find that

$$H(r_H, E) = \frac{12\ell E}{4\ell^2 E + 3r_H^2} > 0. \quad (5.15)$$

Equations (3.37) and (3.38) then tell us that the surface $r = r_H$ is a horizon for a test particle with energy E . It should be noted that, in contrast to the Schwarzschild case studied in Sec. III B 2 [cf. Eq. (3.42)], r_H is now proportional to E ; that is, the higher the energy of the test particle, the larger the radius of the horizon. To understand this, let us consider the acceleration of a test particle with its four-velocity $u_\lambda = -\delta^r_r$, located on a surface r . Then, we find that

$$a_\mu \equiv u_{\mu;\lambda} u^\lambda = \begin{cases} -\frac{m}{r^2} \delta^r_\mu & \text{Schwarzschild} \\ \frac{r}{\ell^2} \delta^r_\mu & \text{de Sitter.} \end{cases} \quad (5.16)$$

That is, for the Schwarzschild solution, the test particle feels an attractive force, while for the de Sitter solution, it feels a repulsive one. Because of this difference, in the de Sitter spacetime r_H is proportional to E , in contrast to

the Schwarzschild one, where it is inversely proportional to E , as shown explicitly in Eq. (3.42).

B. $m > 0, \Lambda = 0$

When $\Lambda = 0$ and $m > 0$, it is the Schwarzschild solution studied in Secs. III B 2 and III C in detail. In particular, in the IR, the surface $r = 2m$ represents a horizon, while for high-energy particles, the radius of the horizon is energy dependent, as explicitly given by Eq. (3.42) for $n = 2$. So, we shall not repeat these studies, but simply note that now the solution takes the form

$$ds^2 = -dt^2 + \left(dr - \sqrt{\frac{2m}{r}} dt\right)^2 + r^2 d\Omega^2, \quad (5.17)$$

which is singular only at $r = 0$, as can be seen from Eq. (5.5). So, it already represents a maximal spacetime in the HL theory.

It is interesting to note that the above metric covers only half of the maximally extended spacetime given in GR. This can be seen easily by introducing the coordinate τ [43],

$$\begin{aligned} \tau &\equiv t - \int \frac{\sqrt{2mr}}{r - 2m} dr \\ &= t - 2\sqrt{2mr} - 2m \ln\left(\frac{r - 2m}{(\sqrt{r} + \sqrt{2m})^2}\right), \end{aligned} \quad (5.18)$$

in terms of which, the solution takes the standard Schwarzschild form $ds^2 = -f(r)d\tau^2 + f^{-1}(r)dr^2 + r^2 d\Omega^2$ with $f(r) = 1 - 2m/r$. Of course, the above transformations are forbidden by Eq. (1.2).

C. $m > 0, \Lambda \neq 0$

In this case, it is convenient to further distinguish the two subcases $\Lambda > 0$ and $\Lambda < 0$.

I. $\Lambda > 0$

In this case, the metric takes the form

$$ds^2 = -dt^2 + \left(dr - \sqrt{\frac{2m}{r} + \frac{r^2}{\ell^2}} dt\right)^2 + r^2 d\Omega^2. \quad (5.19)$$

When $E \ll M_*$, as in the last case the dispersion relation becomes relativistic, and $F(\zeta) \simeq \zeta$, for which we have $n = 1$. Then, we find that

$$H(r) = 1 + N^r = 1 - \sqrt{\frac{2m}{r} + \frac{r^2}{\ell^2}} = \frac{F(r)}{\ell^2(1 + \sqrt{\frac{2m}{r} + \frac{r^2}{\ell^2}})}, \quad (5.20)$$

but now $F(r) \equiv -(r^3 - \ell^2 r + 2m\ell^2)$. Clearly, $F(r)$ has one maximum and one minimum, respectively, at $r = \pm r_m$, where $r_m = \ell/\sqrt{3}$ and $F(r_m) = -2\ell^2(m - 1/(3\sqrt{\Lambda}))$, as shown in Fig. 10. Thus, when $m^2 > 1/(9\Lambda^2)$, $H(r) = 0$ has no real positive root, and a

horizon does not exist even in the IR. Therefore, the singularity at $r = 0$ is naked. When $m^2 < 1/(9\Lambda^2)$, $H(r) = 0$ has two real and positive roots, r_{\pm} ($r_+ > r_-$), where $r = r_+$ is often referred to as the cosmological horizon and $r = r_-$ the black hole event horizon [50]. When $m^2 = 1/(9\Lambda^2)$, the two horizons coincide. In GR, the corresponding Penrose diagrams were given in [50]. However, as argued above, in the HL theory these diagrams are not allowed, as they are obtained by coordinate transformations that violate the restricted diffeomorphisms (1.2). Nevertheless, since the metric is not singular in the current form, it already represents a maximal spacetime.

When $E \gg M_*$, the high momentum terms dominate, and for $n = 2$, we find that

$$\begin{aligned} X(r) &= \frac{2E}{\sqrt{\frac{2m}{r} + \frac{r^2}{\ell^2} + 4E} + \sqrt{\frac{2m}{r} + \frac{r^2}{\ell^2}}}, \\ H(r) &= \sqrt{\frac{2m}{r} + \frac{r^2}{\ell^2}} - 2X = \frac{F(r)}{\Delta(r)}, \end{aligned} \quad (5.21)$$

where $\Delta(r) > 0$ for any $r \in (0, \infty)$, and $F(r) \equiv r^3 - 4E\ell^2 r/3 + 2m\ell^2$. It can be shown that when $m^2 > 8\ell E^{3/2}/27$, $H(r) = 0$ has no real and positive roots. Thus, in this case there are no horizons, and the singularity at $r = 0$ must be naked. When $m^2 < 8\ell E^{3/2}/27$, $H(r) = 0$ has two real and positive roots, say, $r_{1,2}$ ($r_2 > r_1$), but now $r_{1,2} = r_{1,2}(E, m, \ell)$. Thus, in this case there also exists two horizons, but each of them depends on E . When $m^2 = 8\ell E^{3/2}/27$, we have $r_1 = r_2$, and the two horizons coincide.

2. $\Lambda < 0$

In this case, the metric takes the form

$$ds^2 = -dt^2 + \left(dr - \sqrt{\frac{2m}{r} - \frac{r^2}{\ell^2}} dt \right)^2 + r^2 d\Omega^2, \quad (5.22)$$

where $\ell \equiv \sqrt{3/|\Lambda|}$. Then, from Eq. (5.5), it can be seen that the spacetime is singular at $r_s \equiv (2m\ell^2)^{1/3}$ [46]. This is different from GR, in which the only singularity of the anti-de Sitter Schwarzschild solution is at $r = 0$.

When $E \ll M_*$, as in the last case, the dispersion relation becomes relativistic. Then, we find that

$$H(r) = 1 + N^r = 1 - \sqrt{\frac{2m}{r} - \frac{r^2}{\ell^2}} = \frac{F(r)}{r\ell^2(1 + \sqrt{\frac{2m}{r} - \frac{r^2}{\ell^2}})}, \quad (5.23)$$

but now with $F(r) \equiv r^3 + \ell^2 r - 2m\ell^2$, which is a monotonically increasing function, as shown by Fig. 14. Thus, $H(r) = 0$ has one and only one real and positive root, $r_H = r_H(m, \ell)$. But, r_H is always less than r_s , i.e., $r_H < r_s$. Thus, the singularity at $r = r_s$ is a naked singularity.

When $E \gg M_*$, let us consider only the case $n = 2$. Then, we find that

$$\begin{aligned} X(r) &= \frac{2E}{\sqrt{\frac{2m}{r} - \frac{r^2}{\ell^2} + 4E} + \sqrt{\frac{2m}{r} - \frac{r^2}{\ell^2}}}, \\ H(r) &= \sqrt{\frac{2m}{r} - \frac{r^2}{\ell^2}} - 2X = \frac{F(r)}{\Delta(r)}, \end{aligned} \quad (5.24)$$

where $\Delta(r) > 0$ for any $r \in (0, \infty)$, and $F(r) \equiv r^3 + 4E\ell^2 r/3 - 2m\ell^2$. It can be shown that this $F(r)$ is also a monotonically increasing function, as shown by Fig. 14, and $F(r) = 0$ has only one real and positive root, $r_H = r_H(m, E, \ell)$. Again, since $H(r_s) = 1$ and $H(r_H) = 0$, we find that r_H is also always less than r_s , although now r_H depends on E . Thus, the singularity at $r = r_s$ is a naked singularity.

VI. CONCLUSIONS

In this paper, we have systematically studied black holes in the HL theory, using the kinematic method of test particles provided by KK in [38], in which a horizon is defined as the surface at which massless test particles are infinitely redshifted. Because of the nonrelativistic dispersion relations (1.5), in Sec. III we have shown explicitly the difference between black holes defined in GR and the ones defined here. In particular, the radius of the horizon usually depends on the energy of the test particles.

When applying this definition to the spherically symmetric and static vacuum solutions found recently in [22,40,41], in Secs. IV and V we have found that for test particles with sufficiently high energy, the radius of the horizon can be made arbitrarily small, although the singularities at the center can be seen, in principle, only by test particles with infinitely high energy.

In Secs. IV and V, we paid particular attention to the global structures of the static solutions. Because of the restricted diffeomorphisms (1.5), they are dramatically different from the corresponding ones given in GR, although the solutions are the same. In particular, the restricted diffeomorphisms (1.5) do not allow us to draw Penrose diagrams, although one can create something similar to them; for example, see Figs. 3, 5, 9, 12, and 15. But, it must be noted that, since the speed of the test particles in the HL theory can be infinitely large, the causality in this theory is also dramatically different from that of GR [cf. Fig. 1]. In particular, the light-cone structure in GR does not apply to the HL theory. Among the static solutions, a very interesting case is the one given by Fig. 5, which corresponds to an Einstein-Rosen bridge. In GR, this solution is made of an exotic fluid, as one can see from Eq. (4.27), which is clearly unphysical, and most likely unstable, too. However, in the HL theory, the solution is a vacuum one, and it would be very interesting to see if this configuration is stable or not in the HMT setup.

Finally, in Appendix B we have studied the slowly rotating solutions in the HMT setup [22], and explicitly found all such solutions which are characterized by an arbitrary function $A_0(r)$. When $A_0 = 0$ they reduce to the slowly rotating Kerr solution obtained in GR. When the rotation is switched off, they reduce to the static solutions obtained in [41].

ACKNOWLEDGMENTS

J. X. L. would like to thank the Physics Department and CASPER at Baylor University for hospitality during his visit there where part of this work was initiated and completed. Part of this work was also done when two of the authors (J. X. L. and A. W.) attended the advanced workshop ‘‘Dark Energy and Fundamental Theory,’’ Tunxi, China, April 8–18, 2011, supported by the Special Fund

for Theoretical Physics from the National Natural Science Foundation of China (NNSFC), Grant No. 10947203. J. L. acknowledges support from the EPSRC, United Kingdom. J. X. L. acknowledges support from the Chinese Academy of Sciences, a grant from the 973 Program with Grant No. 2007CB815401 and a grant from the NNSFC with Grant No. 10975129. A. W. is supported in part by DOE Grant No. DE-FG02-10ER41692 and NNSFC Grant No. 11075141.

APPENDIX A: THE FUNCTIONS $(F_s)_{ij}$

For the solution

$$\nu = -\frac{1}{2} \ln\left(1 + \frac{C}{r} - \frac{1}{3} \Lambda_g r^2\right), \quad (\text{A1})$$

the functions $(F_s)_{ij}$ appearing in Eq. (2.12) are given by

$$\begin{aligned} (F_0)_{ij} &= -\frac{1}{2} g_{ij} = -\frac{1}{2} e^{2\nu} \delta_i^r \delta_j^r - \frac{1}{2} r^2 \Omega_{ij}, \\ (F_1)_{ij} &= -\frac{1}{2} g_{ij} R + R_{ij} = \frac{e^{2\nu}}{3r^3} (3C - \Lambda_g r^3) \delta_i^r \delta_j^r - \frac{1}{6r} (3C + 2\Lambda_g r^3) \Omega_{ij}, \\ (F_2)_{ij} &= -\frac{1}{2} g_{ij} R^2 + 2RR_{ij} - 2\nabla_{(i} \nabla_{j)} R + 2g_{ij} \nabla^2 R = \frac{2\Lambda_g e^{2\nu}}{3r^3} (6C + \Lambda_g r^3) \delta_i^r \delta_j^r - \frac{2\Lambda_g}{3r} (3C - \Lambda_g r^3) \Omega_{ij}, \\ (F_3)_{ij} &= -\frac{1}{2} g_{ij} R_{mn} R^{mn} + 2R_{ik} R_j^k - 2\nabla^k \nabla_{(i} R_{j)k} + \nabla^2 R_{ij} + g_{ij} \nabla_m \nabla_n R^{mn} \\ &= \frac{e^{2\nu}}{36r^6} (-9C^2 + 60C\Lambda_g r^3 + 8\Lambda_g^2 r^6) \delta_i^r \delta_j^r + \frac{1}{18r^4} (9C^2 - 15C\Lambda_g r^3 + 4\Lambda_g^2 r^6) \Omega_{ij}, \\ (F_4)_{ij} &= -\frac{1}{2} g_{ij} R^3 + 3R^2 R_{ij} - 3\nabla_{(i} \nabla_{j)} R^2 + 3g_{ij} \nabla^2 R^2 = \frac{4\Lambda_g^2 e^{2\nu}}{r^3} (3C + \Lambda_g r^3) \delta_i^r \delta_j^r - \frac{2\Lambda_g^2}{r} (3C - 2\Lambda_g r^3) \Omega_{ij}, \\ (F_5)_{ij} &= -\frac{1}{2} g_{ij} RR^{mn} R_{mn} + R_{ij} R^{mn} R_{mn} + 2RR_{ki} R_j^k - \nabla_{(i} \nabla_{j)} (R^{mn} R_{mn}) - 2\nabla^n \nabla_{(i} RR_{j)n} + g_{ij} \nabla^2 (R^{mn} R_{mn}) + \nabla^2 (RR_{ij}) \\ &\quad + g_{ij} \nabla_m \nabla_n (RR^{mn}) \\ &= \frac{e^{2\nu}}{6r^9} (-99C^3 + 39C^2 \Lambda_g r^3 - 108C^2 r + 28C\Lambda_g^2 r^6 + 8\Lambda_g^3 r^9) \delta_i^r \delta_j^r + \frac{1}{12r^7} (693C^3 - 156C^2 \Lambda_g r^3 \\ &\quad + 648C^2 r - 28C\Lambda_g^2 r^6 + 16\Lambda_g^3 r^9) \Omega_{ij}, \\ (F_6)_{ij} &= -\frac{1}{2} g_{ij} R_n^m R_p^n R_m^p + 3R^{mn} R_{ni} R_{mj} + \frac{3}{2} \nabla^2 (R_{in} R_j^n) + \frac{3}{2} g_{ij} \nabla_k \nabla_l (R_n^k R^{ln}) - 3\nabla_k \nabla_{(i} (R_{j)n} R^{nk}) \\ &= \frac{e^{2\nu}}{36r^9} (-675C^3 + 270C^2 \Lambda_g r^3 - 729C^2 r + 72C\Lambda_g^2 r^6 + 16\Lambda_g^3 r^9) \delta_i^r \delta_j^r \\ &\quad + \frac{1}{72r^7} (4725C^3 - 1080C^2 \Lambda_g r^3 + 4374C^2 r - 72C\Lambda_g^2 r^6 + 32\Lambda_g^3 r^9) \Omega_{ij}, \\ (F_7)_{ij} &= \frac{1}{2} g_{ij} (\nabla R)^2 - (\nabla_i R) (\nabla_j R) + 2R_{ij} \nabla^2 R - 2\nabla_{(i} \nabla_{j)} \nabla^2 R + 2g_{ij} \nabla^4 R = 0, \\ (F_8)_{ij} &= -\frac{1}{2} g_{ij} (\nabla_p R_{mn}) (\nabla^p R^{mn}) - \nabla^4 R_{ij} + (\nabla_i R_{mn}) (\nabla_j R^{mn}) + 2(\nabla_p R_{in}) (\nabla^p R_j^n) + 2\nabla^n \nabla_{(i} \nabla^2 R_{j)n} + 2\nabla_n (R_m^n \nabla_{(i} R_{j)}^m) \\ &\quad - 2\nabla_n (R_{m(j} \nabla_{i)} R^{mn}) - 2\nabla_n (R_{m(i} \nabla^n R_{j)}^m) - g_{ij} \nabla^n \nabla^m \nabla^2 R_{mn} \\ &= \frac{C e^{2\nu}}{12r^9} (180C^2 - 75C\Lambda_g r^3 + 189Cr - 4\Lambda_g^2 r^6) \delta_i^r \delta_j^r + \frac{C}{12r^7} (-630C^2 + 150C\Lambda_g r^3 - 567Cr + 2\Lambda_g^2 r^6) \Omega_{ij}, \quad (\text{A2}) \end{aligned}$$

where $\Omega_{ij} \equiv \delta_i^\theta \delta_j^\theta + \sin^2 \theta \delta_i^\phi \delta_j^\phi$.

APPENDIX B: SLOWLY ROTATING VACUUM SOLUTIONS

Slowly rotating vacuum solutions in other versions of the HL theory have been studied by several authors [51]. The goal of this section is to derive slowly rotating black hole solutions in the HMT setup. We will seek a solution of the form

$$ds^2 = -dt^2 + r^2(d\theta^2 + \sin^2\theta d\phi^2) + e^{2\nu(r)}[dr + e^{\mu(r)-\nu(r)}(dt - a\omega(r)\sin^2\theta d\phi)]^2, \quad (\text{B1})$$

where the functions $\nu(r)$, $\mu(r)$, and $\omega(r)$ are independent of (t, θ, ϕ) . By requiring that the metric satisfy the equations to first order in the small rotation parameter a , we will be able to determine ν , μ , and ω .

The ansatz (B1) is motivated by the fact that it agrees with the Kerr solution to first order in a . Indeed, the Kerr line element expressed in Doran coordinates [52] is given by

$$ds_{\text{Kerr}}^2 = -dt^2 + (r^2 + a^2\cos^2\theta)d\theta^2 + (r^2 + a^2)\sin^2\theta d\phi^2 + \frac{r^2 + a^2\cos^2\theta}{r^2 + a^2} \times \left[dr + \frac{\sqrt{2mr(r^2 + a^2)}}{r^2 + a^2\cos^2\theta}(dt - a\sin^2\theta d\phi) \right]^2, \quad (\text{B2})$$

where m and a are parameters. As $a \rightarrow 0$, this metric coincides with (B1) to first order in the rotation parameter a , provided that

$$\nu(r) = 0, \quad \mu(r) = \log\sqrt{\frac{2m}{r}}, \quad \omega(r) = 1.$$

In particular, when $a = 0$, it reduces to the Schwarzschild metric in Painlevé-Gullstrand form.

Note that the form (B1) of the line element is compatible with the projectability condition $N = N(t)$; its Arnowitt-Deser-Misner coefficients are

$$N = 1, \quad N^i = (e^{\mu(r)-\nu(r)}, 0, 0).$$

Working in the gauge $\varphi = 0$, the momentum constraint (2.6) for the metric (B1) reduces to

$$-\frac{2e^{\mu-3\nu}\nu'}{r} + O(a^2) = 0, \\ \frac{ae^{2\mu-2\nu}}{2r^4} [r^2(\omega'' + \omega'(4\mu' - \nu')) - 2\omega(1 - r^2\mu'' + r^2\mu'\nu' - 2r^2\mu'^2 + r\nu')] + O(a^2) = 0, \quad (\text{B3})$$

while Eq. (2.9) obtained from variation with respect to A yields

$$(1 - r^2\Lambda_g)e^{2\nu} + 2r\nu' - 1 + O(a^2) = 0. \quad (\text{B4})$$

The first equation in (B3) implies that ν is constant, and then (B4) shows that

$$\nu = 0, \quad \Lambda_g = 0.$$

This yields

$$R_{ij} = O(a^2), \\ \mathcal{L}_K = -\frac{2}{r^2}e^{2\mu}(1 + 2r\mu') + O(a^2), \\ \mathcal{L}_V = 2\Lambda + O(a^2). \quad (\text{B5})$$

The (rr) component of the dynamical equations (2.11) gives

$$\frac{2rA_0' - r^2\Lambda + 2re^{2\mu}\mu' + e^{2\mu}}{r^2} + \frac{2A_1'}{r}a + O(a^2) = 0, \quad (\text{B6})$$

where we have assumed that $A(r)$ has the form

$$A(r) = A_0(r) + A_1(r)a + O(a^2). \quad (\text{B7})$$

The terms of $\mathcal{O}(1)$ in (B6) imply that

$$\mu(r) = \frac{1}{2} \ln\left(\frac{2m}{r} + \frac{1}{3}r^2\Lambda - 2A_0(r) + \frac{2}{r} \int_{r_0}^r A_0(s)ds\right), \quad (\text{B8})$$

where $r_0 > 0$ is a constant, while the terms of $\mathcal{O}(a)$ imply that A_1 is a constant. With these choices, all the components of the dynamical equations, as well as the equations obtained from variation with respect to A and φ , are satisfied to first order in a , and the Hamiltonian constraint (2.5) becomes

$$\int_0^\infty rA_0'(r)dr + O(a^2) = 0.$$

Finally, the second equation in the momentum constraint (B3) is satisfied to $\mathcal{O}(a)$ provided that

$$\omega(r) = e^{-2\mu}\left(\frac{d_1}{r} + d_2r^2\right) = \frac{d_1 + d_2r^3}{2m + 2 \int_{r_0}^r A_0(s)ds - 2rA_0 + \frac{\Lambda}{3}r^3}, \quad (\text{B9})$$

where d_1 and d_2 are the integration constants.

In summary, the ansatz (B1) gives a solution to first order in a provided that $\mu(r)$ is given by (B8), $\omega(r)$ is given by (B9), and

$$\nu = 0, \quad A(r) = A_0(r) + aA_1 + O(a^2), \quad (\text{B10})$$

where $r_0 > 0$, m , Λ , A_1 , d_1 , d_2 are arbitrary constants, and $A_0(r)$ can be freely chosen as long as

$$\int_0^\infty rA_0'(r)dr = 0.$$

We recover the slowly rotating version of the Kerr solution by taking $A_0 = 0$, $\Lambda = 0$, and $d_2 = 0$. Setting $a = 0$, on the other hand, we recover the static solutions obtained in [41].

Let us point out that the standard Einstein equations also allow for a nonzero value of d_2 in the slowly rotating limit. Indeed, substituting the ansatz (B1) with $\nu = 0$ into the vacuum Einstein equations

$$R_{\alpha\beta} - \frac{1}{2}g_{\alpha\beta}R = 0, \quad \alpha, \beta = 0, 1, 2, 3,$$

we find that they are satisfied to order $\mathcal{O}(a)$ if and only if

$$\mu(r) = \frac{1}{2} \ln\left(\frac{2m}{r}\right),$$

where $m > 0$ is a constant, and $\omega(r)$ is given by (B9) with arbitrary constants d_1 and d_2 .

-
- [1] P. Horava, *Phys. Rev. D* **79**, 084008 (2009).
 [2] E. M. Lifshitz, *Zh. Eksp. Teor. Fiz.* **11**, 255 (1941); **11**, 269 (1941).
 [3] E. Kiritsis and G. Kofinas, *Nucl. Phys.* **B821**, 467 (2009).
 [4] G. Calcagni, *J. High Energy Phys.* 09 (2009) 112.
 [5] R. Brandenberger, *Phys. Rev. D* **80**, 043516 (2009).
 [6] A. Wang and Y. Wu, *J. Cosmol. Astropart. Phys.* 07 (2009) 012.
 [7] S. Mukohyama, *J. Cosmol. Astropart. Phys.* 06 (2009) 001.
 [8] Y.-S. Piao, *Phys. Lett. B* **681**, 1 (2009); B. Chen, S. Pi, and J.-Z. Tang, *J. Cosmol. Astropart. Phys.* 08 (2009) 007.
 [9] K. Yamamoto, T. Kobayashi, and G. Nakamura, *Phys. Rev. D* **80**, 063514 (2009).
 [10] A. Wang and R. Maartens, *Phys. Rev. D* **81**, 024009 (2010).
 [11] A. Wang, D. Wands, and R. Maartens, *J. Cosmol. Astropart. Phys.* 03 (2010) 013.
 [12] S. Mukohyama, *Classical Quantum Gravity* **27**, 223101 (2010).
 [13] T.P. Sotiriou, *J. Phys. Conf. Ser.* **283**, 012034 (2011).
 [14] A. Padilla, *J. Phys. Conf. Ser.* **259**, 012033 (2010).
 [15] P. Horava, *Classical Quantum Gravity* **28**, 114012 (2011).
 [16] M. Visser, arXiv:1103.5587.
 [17] A. Borzou, K. Li, and A. Wang, *J. Cosmol. Astropart. Phys.* 05 (2011) 006.
 [18] D. Blas, O. Pujolas, and S. Sibiryakov, *Phys. Rev. Lett.* **104**, 181302 (2010); *J. High Energy Phys.* 04 (2011) 018.
 [19] M. Li and Y. Pang, *J. High Energy Phys.* 08 (2009) 015; M. Henneaux, A. Kleinschmidt, and G.L. Gmez, *Phys. Rev. D* **81**, 064002 (2010).
 [20] J. Kluson, *Phys. Rev. D* **83**, 044049 (2011); arXiv:1101.5880; J. Kluson, S. Nojiri, S.D. Odintsov, and D. Saez-Gomez, *Eur. Phys. J. C* **71**, 1690 (2011).
 [21] I. Kimpton and A. Padilla, *J. High Energy Phys.* 07 (2010) 014.
 [22] P. Horava and C.M. Melby-Thompson, *Phys. Rev. D* **82**, 064027 (2010).
 [23] A. Wang and Y. Wu, *Phys. Rev. D* **83**, 044031 (2011).
 [24] A.M. da Silva, *Classical Quantum Gravity* **28**, 055011 (2011).
 [25] Y.-Q. Huang and A. Wang, *Phys. Rev. D* **83**, 104012 (2011).
 [26] C. Charmousis, G. Niz, A. Padilla, and P.M. Saffin, *J. High Energy Phys.* 08 (2009) 070; K. Koyama and F. Arroja, *J. High Energy Phys.* 03 (2010) 061; A. Papazoglou and T.P. Sotiriou, *Phys. Lett. B* **685**, 197 (2010).
 [27] D. Blas, O. Pujolas, and S. Sibiryakov, *J. High Energy Phys.* 10 (2009) 029.
 [28] A. Wang and Q. Wu, *Phys. Rev. D* **83**, 044025 (2011).
 [29] T. Sotiriou, M. Visser, and S. Weinfurter, *Phys. Rev. Lett.* **102**, 251601 (2009); *J. High Energy Phys.* 10 (2009) 033; *J. Phys. Conf. Ser.* **222**, 012054 (2010).
 [30] A.I. Vainshtein, *Phys. Lett.* **39B**, 393 (1972).
 [31] B. Chen and Q.G. Huang, *Phys. Lett. B* **683**, 108 (2010).
 [32] S.W. Hawking and G.F.R. Ellis, *The Large Scale Structure of Space-Time*, Cambridge Monographs on Mathematical Physics (Cambridge University Press, Cambridge, England, 1973).
 [33] F.J. Tipler, *Nature (London)* **270**, 500 (1977).
 [34] S.A. Hayward, *Phys. Rev. D* **49**, 6467 (1994); *Classical Quantum Gravity* **17**, 1749 (2000).
 [35] A. Wang, *Phys. Rev. D* **68**, 064006 (2003); **72**, 108501 (2005); *Gen. Relativ. Gravit.* **37**, 1919 (2005); A.Y. Miguelote, N.A. Tomimura, and A. Wang, *ibid.* **36**, 1883 (2004); P. Sharma, A. Tziolas, A. Wang, and Z.-C. Wu, *Int. J. Mod. Phys. A* **26**, 273 (2011).
 [36] P. Horava and C.M. Melby-Thompson, *Gen. Relativ. Gravit.* **43**, 1391 (2010).
 [37] T. Suyama, *J. High Energy Phys.* 01 (2010) 093; D. Capasso and A. P. Polychronakos, *ibid.* 02 (2010) 068; J. Alexandre, K. Farakos, P. Pasipoularides, and A. Tsalpalis, *Phys. Rev. D* **81**, 045002 (2010); J.M. Romero, V. Cuesta, J.A. Garcia, and J.D. Vergara, *ibid.* **81**, 065013 (2010); S.K. Rama, arXiv:0910.0411; L. Sindoni, arXiv:0910.1329.
 [38] E. Kiritsis and G. Kofinas, *J. High Energy Phys.* 01 (2010) 122.
 [39] E. Barausse, T. Jacobson, and T.P. Sotiriou, *Phys. Rev. D* **83**, 124043 (2011); T. Jacobson, *Phys. Rev. D* **81**, 101502 (2010); **82**, 129901(E) (2010).
 [40] J. Alexandre and P. Pasipoularides, *Phys. Rev. D* **83**, 084030 (2011).
 [41] J. Greenwald, V.H. Satheeshkumar, and A. Wang, *J. Cosmol. Astropart. Phys.* 12 (2010) 007.
 [42] A. Wang, *Phys. Rev. D* **82**, 124063 (2010).
 [43] J. Greenwald, A. Papazoglou, and A. Wang, *Phys. Rev. D* **81**, 084046 (2010).
 [44] R.G. Cai, L.M. Cao, and N. Ohta, *Phys. Rev. D* **80**, 024003 (2009); A. Kehagias and K. Sfetsos, *Phys. Lett. B* **678**, 123 (2009); M.-i. Park, *J. High Energy Phys.* 09 (2009) 123; A. Ghodsi and E. Hatefi, *Phys. Rev. D* **81**,

- 044016 (2010); K. Izumi and S. Mukohyama, *ibid.* **81**, 044008 (2010); E. Kiritsis, *ibid.* **81**, 044009 (2010); G. Koutsoumbas, E. Papantonopoulos, P. Pasipoularides, and M. Tsoukalas, *ibid.* **81**, 124014 (2010), and references therein.
- [45] P. Painleve, C. R. Acad. Sci. (Paris) **173**, 677 (1921); A. Gullstrand, Ark. Mat. Astron. Fys. **16**, 1 (1922).
- [46] R.-G. Cai and A. Wang, *Phys. Lett. B* **686**, 166 (2010).
- [47] C. W. Misner, K. S. Thorne, and J. A. Wheeler, *Gravitation* (W. H. Freeman and Company, San Francisco, 1973), pp. 484–528.
- [48] M. Visser, *Lorentzian Wormholes* (AIP Press, New York, 1996).
- [49] T. Ha *et al.*, [arXiv:0905.0396](https://arxiv.org/abs/0905.0396).
- [50] G. W. Gibbons and S. W. Hawking, *Phys. Rev. D* **15**, 2738 (1977).
- [51] A. N. Aliev and C. Sentürk, *Phys. Rev. D* **82**, 104016 (2010); H. W. Lee, Y. W. Kim, and Y. S. Myung, *Eur. Phys. J. C* **70**, 367 (2010); A. Ghodsi and E. Hatefi, *Phys. Rev. D* **81**, 044016 (2010).
- [52] C. Doran, *Phys. Rev. D* **61**, 067503 (2000).